Response to NRC Comment #5- Revised EIS

The reviewer makes several comments about the applicability of conceptual model and the groundwater numerical model. These include concerns about the overall calibration of the model to steady state conditions related to:

- The simulation of the aquitard;
- the adequacy of the groundwater flow model to predict dewatering requirements;
- the adequacy of the groundwater flow model to predict regional effects; and,
- Use of shaft inflow data.

As the reviewer notes, calibration to steady state conditions have improved since the draft EIS by inclusion of results from the 20-day prototype dewatering well pump test but continues on to suggest that the calibration of model to steady state still needs to be improved. Shore believes that as described below, the calibration differences are due to complex local geology near the kimberlites, and does not introduce error in regional predictions or estimation of dewatering requirements or represent poor understanding of the flow system.

***Simulation of the aquitard***

Steady-state calibration within the tills and Colorado group shales near the kimberlites is not as good as calibration further away from the kimberlites and in other formations. The reviewer suggests that this could be due to a thin layer of permeable material (basal till of the Empress group) at the till-Colorado group interface. Although this is a possible explanation for the calibration, extensive drilling conducted during exploration indicates that, when present, the basal till layer is discontinuous and heterogeneous. A detailed description of the till-shale contact geology around Orion South is included in the file (NRCan #5 Basal Till Note_2012-09-21.pdf). At Star, these basal layers are not present in the core drilling. These drilling results suggest that incorporation of such a variable feature with significant local discontinuity is not justified in a regional groundwater model is not justified. Shore agrees with the reviewer that, from the calibration, that the regional hydrogeology is better represented in the model, whereas the site specific hydrogeology (i.e., near the kimberlites) is less well represented.

Prior to getting this comment, Shore noticed kimberlite lenses within the shale aquitard adjacent to kimberlite bodies. As such, in order to gain a better understanding of the local hydrogeology, specifically the confining layer, Shore commissioned the University of Saskatchewan to study the properties of the Colorado Group shale. The U of S paper (Schmeling and Hendry 2013) is attached as part of the answer to this information request, as NRC #5 A Transport of Natural Tracers.pdf and NRC #5 B Transport paper figures Jan 8 2013.pdf. The U of S study looked at two core holes, one near the kimberlites (referred to as a geologically complex shale due to interactions with kimberlite) and one away from the kimberlites (referred to as geologically simple shale). Using natural tracers, the authors concluded that molecular diffusion dominated water movement through not only the undisturbed shale, but also

through about 50 m into the upper Mannville formation. Schmeling and Hendry (2013) estimated a vertical hydraulic conductivity (Kv) of 8·10-12 m s-1 for the shale based on maximum velocities and observed gradient in areas away from the kimberlites and in undisturbed shale near the kimberlite. In the more complex area near the kimberlites, advective processes dominated water movement in zones influenced by kimberlite emplacement, however Kv values above the fractured zone and below were similar to those outside of the influence of the kimberlite.

This local complexity adjacent to the kimberlite is likely responsible for the overprediction of heads at Star West, and potentially at Orion North, and it is rather unlikely that the overprediction is a result of a lack of regional understanding of the aquitards.

In addition, the U of S calculated kv is lower than the values used in 2011 SRK modeling (SRK used a Kv of 0.0006 m/d or 6.9 x 10-10 m/s for the shale), Since SRK's sensitivity analysis that showed that surficial impacts are very sensitive to kv, using a high kv in the model is conservative and likely overestimates shallow groundwater affects. Observations by the U of S also and help to explain some of the variability and difficulty when comparing data from transducers in the Colorado group shale near the kimberlites.

**Prediction of Dewatering Requirements**

Determination of the Project dewatering requirements and diffuser capacity are driven primarily by the permeabilities in the confined Mannville aquifer which are well understood and which was also refined using the results of the long-term 20-day pump test. This pumping test was conducted at 900 gallons per minute and managed to significantly stress the aquifer so that vertical differences in the Mannville aquifer were evident.. Mannville aquifer heads in the groundwater flow model are reasonably predicted in both near field and far field piezometers (See File NRC #5 GWModel calibration.pdf), further supporting the dewatering simulations.

Calibration of the groundwater flow model to absolute values of head in the shale and overlying units, , is not significant to calculation of dewatering requirements that simulating the vertical gradient. At the two sites where there is significant data, the vertical hydraulic gradient both within the shale and between the shale and Mannville Aquifer are reasonably well calibrated. For predicting dewatering and impacts, a reasonable representation of the gradient driving groundwater movement is more important that simulating the absolute values of levels in the various units. In summary due the knowledge of the Mannville Aquifer that was put into the 2011 SRK model and the fact the head in the Mannville and the gradient in the overlying units are well simulated, Shore believes that the prediction of the dewatering requirement is reasonable and is suitable for assessing impacts.

**Prediction of Regional Effects**

As demonstrated by the sensitivity analyses, drawdown in surficial aquifers is sensitive to the vertical hydraulic conductivity (Kv) in the till, shale and upper Mannville aquifer. In the revised model, the Kv of the confining layer is about two orders of magnitude greater than the kvdetermined by the U of S study (Schmeling and Hendry, 2011). In addition, the presented sensitivity analysis shows that model calibration becomes worse when more conductive values are used. Within the model, Kv's from near

the kimberlites are more conductive than regional values, as discussed above likely due to effects of the kimberlite stringers and lenses adjacent to the kimberlites bodies. The regional and kimberlite influenced Kv's were averaged and then used in the regional model. The application of this average Kv is conservative since the average value is more than the regional Kv that has been measured away from the kimberlite bodies

As described above, kimberlite emplacement has created a very complex local geological setting for the proposed mine. Within the Revised EIS groundwater model, kimberlite deposits were incorporated as a higher conductivity features intruding within the shale based on the magnetic outlines of the deposit. So the effect of the main kimberlite bodies was simulated in the model. So although, the U of S study suggests that the zone of influence of the kimberlites extends beyond the magnetic outlines of these bodies, the effect of these kimberlite lenses or stringers on the responses from the kimberlite bodies would be expected to be variable. Any revision to the groundwater model would only be accomplished by extending the kimberlite effects locally outside of the magnetic signature. This small local change would not change dewatering predictions (as described above) nor would it change impact predictions, since a skin of kimberlite is already being modeled to remain around both open pits. In addition, during operations, the entirety of the kimberlite areas would be dry, as the groundwater levels within the Mannville and the Colorado Group shales near the open pits would be near the bottom of th pit and therefore the water levels would be below these features (SRK, 2011), thus the local poor calibration to water levels in the shale adjacent to the pit does not affect regional impact predictions and /or the potential dewatering rates. Additional information may be obtained during detailed design prior or during operations and the groundwater model will be updated on a regular basis, the model presented in the Revised EIS is conservative, based on a good understanding of the regional geology and likely over predicts regional drawdown by applying an average Kv to the entire Colorado group shale

***Shaft Inflows***

Shore has previously examined the idea of using the mine and shaft inflow rates for model calibration. This idea was proven not to be possible for the following rasons:

- the shafts and the levels were all lined with grout at both Star and Orion South.
- during the test mining at Star, the levels intersected the Mannville formation on at least two locations.

So although a maximum inflow into the former Star test mine workings was estimated for other purposes, this flow estimate were not used in the groundwater flow model as there was no way to assign the flow to a specific geological unit and/or to remove the effect of the grout lining

***Conclusion***

Shore believes that the above discussions and the existing geological and hydrogeological information indicate that the groundwater model is based on a good understanding of the regional geologic setting. The information in the SRK groundwater model are supported by 20-day high flow pumping test and the U of S testing. Analyses of both these information sources have improved our understanding and help to confirm our conceptual model of the complex geological setting near the Star and Orion South kimberlites. As a result Shore can reasonably conclude that, despite less than ideal calibration to steady state conditions, the model conservatively predicts effects of dewatering on surficial aquifers and also on dewatering rates thaqt will be encountered during this project.

# Transport of Natural Tracers ($\delta^2$H and Cl) in a Fractured Cretaceous Shale, Fort á la Corne, Saskatchewan, Canada

Erin E. Schmeling[a] and M. Jim Hendry[a],

[a]Department of Geological Sciences, University of Saskatchewan, Saskatoon, SK, Canada

Corresponding Author: Erin E. Schmeling, Department of Geological Sciences, University of Saskatchewan, Saskatoon, SK, Canada, S7N 5E2; e-mail ees423@mail.usask.ca; phone 306-966-5736; fax 306-966-8593

**Abstract**

High-resolution, 1-D vertical profiles of $\delta^2H$ and Cl were collected from two drillholes (203 and 353 m deep) in the Fort á la Corne kimberlite field, Saskatchewan, Canada, to define the vertical controls on solute transport in a geologically simple and geologically complex Cretaceous shale. The complex shale was highly fractured and altered by kimberlite volcanism during deposition (99 to 112 Ma BP) whereas the simple shale appeared to be undisturbed. 1-D profiles and associated transport modeling from the geologically simple corehole suggest diffusion is the dominant transport mechanism through the entire thickness of the Lower Colorado shale aquitard (330 to 246 m above sea level (asl)). In contrast, profiles and associated modeling suggest advection is the dominant transport mechanism through the complex Cretaceous shale (327 to 291 m asl). Below the complex shale, the profiles and modeling suggest diffusion is again the dominant transport process (291 to 191 m asl). Transport modeling of the diffusion-dominated profiles reflects the timing of till deposition, recharge of modern water into the underlying Mannville aquifer, and the onset of the Holocene (390 to 370 ka, 10 to 20 ka, and 10 ka, respectively).

Keywords: fractured aquitard, kimberlite, diffusion, tracers, Canada

## 1. Introduction

Clay-rich deposits (aquitards) are widespread throughout the world and are important for long-term containment of waste and for protecting underlying aquifers from contamination (Gautschi 2001; Hendry and Wassenaar 1999, 2000; Koroleva et al. 2011; Mazurek et al. 2011). As such, knowledge of solute transport and groundwater flow processes in aquitards is important. Natural tracer profiles in clay-rich aquitard formations can be considered large-scale, long-term experiments that can help constrain transport properties over great distances and long time frames (Hendry and Wassenaar 1999; Mazurek et al. 2011).

Early work on natural tracers in clay-rich aquitards focussed on Quaternary deposits (Desaulniers et al. 1981; Hendry and Wassenaar 1999, 2000). More recently studies addressed thick glacial till and unfractured bedrock shale aquitards (Hendry and Wassenaar 1999; Hendry et al. 2011) and deep, indurated, fractured shale deposits (Gautschi 2001; Koroleva et al. 2011; Mazurek et al. 2009, 2011;

Rübel et al. 2002). These studies used a variety of conservative and non-conservative tracers to explore long-term transport mechanisms and the hydrogeological evolution of the aquitard systems. In these cases, both the shape (curvilinear) of 1-D vertical natural tracer profiles with depth and modeling were used to demonstrate that diffusion is the dominant transport mechanism, even in systems in which the aquitard is fractured (Gimmi et al. 2007; Koroleva et al. 2011; Mazurek et al. 2011; Patriarche et al. 2004). In contrast, vertically constant solute profiles may suggest advection is the dominant transport mechanism (Hendry et al. 2004; Kelln et al. 2001). Mathematical modeling of depth tracer profiles can provide estimates of the timing of palaeo-hydrogeologic events, which have been used to test the effect of adding an advective component of transport to the modelled best-fit diffusion profiles (Hendry and Wassenaar 1999, 2000; Hendry et al. 2011; Koroleva et al. 2011; Mazurek et al. 2011). Interpretation of 1-D vertical profiles can also provide an increased level of confidence to physical hydrogeological studies (e.g., K, hydraulic gradients, porosities, recharge rates) of a groundwater system (Hendry and Wassenaar 2011; Remenda et al. 1996).

Groundwater flow in most indurated bedrock shales is limited and occurs mainly in secondary structures such as faults and fractures, if at all (Mazurek et al. 1998). In a study of the hydraulic properties of the Opalinus clay at Mont Terri, Croisé et al. (2004) observed no significant variations in hydraulic conductivity (K) among the different facies and no apparent enhancement of K in the vicinity of tectonic features. Diffusion is also the dominant transport mechanism through the shale at Mont Terri (Mazurek et al. 2011), despite the regional fault system in the Opalinus clay, and at Mont Russelin, Switzerland (Koroleva et al. 2011), despite a complex system of thrust faults. Similarly, in the Opalinus clay at Benken, Switzerland, advective flow is not evident and transport to the underlying aquifer can be explained by diffusion. Conversely, Patriarche et al. (2004) indicate that the $\delta^2H$ profile at Aveyron, France, cannot be explained by diffusion alone and that heterogeneities, such as fractures, have an important role in the development of the tracer profile.

The objective of this investigation was to characterize the groundwater flow and solute transport mechanisms in a geologically simple aquitard site and a geologically complex aquitard site in the same study area. The simple site consists of undisturbed Cretaceous shale deposits. At the complex site, the

Cretaceous shale deposits are highly fractured, being impacted by kimberlite volcanism during deposition. The objective was attained by: (1) obtaining high-resolution vertical profiles of porewater $\delta^2H$ and $\delta^{18}O$ and Cl through both the simple and complex aquitard systems, (2) identifying hydrogeological zones with depth in both systems using the high-resolution profiles; (3) measuring the groundwater age date of the underlying regional aquifer using $^{14}C$ analysis on dissolved inorganic carbon (DIC), and (4) mathematical modeling of the vertical profiles to define the dominant transport mechanism(s) and estimate the paleo-hydrogeologic evolution of the aquitard systems. The current study builds on findings of a companion study that defined the hydrogeology of both the complex and simple systems by characterizing the geotechnical parameters (i.e., dry density [$\rho_d$], bulk density [$\rho$], and gravimetric water content [$\omega$]) of the aquitard and aquifer system as well as estimating K, specific storage (Ss), hydraulic gradients ($i$), and groundwater flow direction in the shale aquitard and the underlying aquifer (Schmeling 2012) (discussed in Section 2, below).

## 2. Study Area and Regional Hydrogeology

This study was conducted on the Shore Gold Inc. exploration site, approximately 60 km east of Prince Albert, Saskatchewan (53°15”N, 104°48” W) (Figure 1). The study area covers about 90 $km^2$ and is bounded by the Saskatchewan River to the south. It is comprised of rolling glacial topography with sandy river sediments ranging in elevation from 360 to 450 m. Several small tributaries drain the site, flowing south towards the Saskatchewan River (Ewert et al. 2009).

The Quaternary glacial sediments at the study site range in thickness from 40 m (near the Saskatchewan River) to 120 m at areas of higher elevation (Figure 2). Both Saskatoon Group (deposited 12 to 500 ka Before Present (BP)) and Sutherland Group (deposited 500 to 2500 ka BP) glacial tills were identified in the region by Christiansen and Sauer (1993). In the study area, the Sutherland Group is about 10 m thick and composed mainly of till (Christiansen and Sauer 1993; Ugorets and Pereira 2011). The Saskatoon Group is generally divided into the Battleford and Floral Formations, both of which consist of a heterogeneous mixture of sand, silt, clay, and coarse-grained sediments up to 75 m thick that are difficult to differentiate. To date, the presence of Battleford till has not been recognized in the study area, although Christiansen and Sauer (1993) suggest Battleford till exists near Prince Albert, Saskatchewan,

60 km to the west. The glacier that deposited the Battleford till near Prince Albert retreated between 10 and 12 ka BP (Christiansen 1978). Holocene (<12 ka BP) proglacial lacustrine and deltaic deposits up to 50 m thick overlie the glacial till units (Christiansen 1978). An intertill sand and gravel aquifer within the Saskatoon Group sediments is also observed within the study area (Schmeling et al. 2012). The Quaternary sediments unconformably overlie about 80-90 m of shale of the Lower Colorado Group and about 150 m of sand, silt, and shale of the Mannville Group (Zonneveld et al. 2004). Schmeling (in prep) document a 60 m thick low K unit within the Mannville (termed upper Mannville) and a 90 m thick high K unit (termed lower Mannville). Both the Lower Colorado and Mannville Group sediments were deposited during the Late Cretaceous (99-112 Ma BP; Zonneveld et al. 2004).

During deposition of both Lower Colorado and Mannville Group sediments, over 70 kimberlite volcanoes erupted into the area. Most of the kimberlites were deposited between 99 and 101 Ma BP (McNeil and Gilboy 2000; Figure 1) in a two-stage process, beginning with the excavation of the crater and subsequent infilling by pyroclastic material (Berryman et al. 2004; Scott-Smith et al. 1998). The size and shape of the craters indicate these processes were powerful, causing fragmentation of the surrounding sediments and volcanically-induced faulting (Lefebvre and Kurszlauskis 2008; Zonneveld et al. 2007). Kimberlite debris flow (KDF) deposits were also formed when walls of the kimberlite volcanoes, comprised of unconsolidated Lower Colorado mudstone, became unstable, slumped, and resedimented on the crater floor, resulting in mixed, deformed, and brecciated kimberlite and shale deposits (Pittari et al. 2006; Zonneveld et al. 2004).

Results of a companion study (Schmeling in prep) suggest that where kimberlite is observed at drillholes in the study area there is a zone of fractured Lower Colorado shale and kimberlite deposits, resulting from kimberlite emplacement. The Lower Colorado shale and kimberlite deposits observed at these drillholes were found to have field scale $K_v$ 1 to 2 orders of magnitude greater than laboratory triaxial $K_v$ measurements, suggesting the presence of transmissive fractures in the kimberlite affected zone. This zone of fractured shale was, however, not observed in drillholes located more than 2 km from the kimberlite bodies, suggesting the presence of both fractured and unfractured shale at the same study area.

Water level measurements through the Quaternary deposits and Lower Colorado and Mannville Group sediments in the study area indicate a strong downward vertical hydraulic gradient from the water table to the Saskatoon Group intertill aquifer as well as an upward vertical gradient from the Mannville, through the Lower Colorado shale and Sutherland Group till, to the Saskatoon intertill aquifer, which acts as a drain. Additional details on the geology and hydrogeology of the study area are presented in Schmeling (in prep).

## 3. Methodology

### *3.1 Sample Collection*

Continuous cores were collected from two coreholes in April and May 2010, using a Boart Longyear diamond drill rig with an HQ (65 mm) core barrel. Borehole 140-10-087 intersected kimberlite within the Lower Colorado shale (i.e., the complex, fractured aquitard system) whereas borehole OVB-10-207 did not (i.e., the geologically simple system) (Figure 1). Core samples were collected from 401 to 93 m asl from 140-10-087 and from 410 to 239 m asl in OVB-10-207. Geological logging of the cores was performed immediately after drilling. The rotary drill mud was spiked with 99% $D_2O$ to a value of up to -30‰. Drill mud and fluid samples were collected every 6 hours during drilling to assess the extent of core contamination by the drilling fluid. These samples (n=32) were collected and stored at room temperature in 250 mL high-polyethylene (HDPE) bottles for stable isotope analyses.

Samples (7.5 cm in diam. x 10-20 cm long; n =303) were collected every 1 m (where core recovery permitted), trimmed to remove the outer 2-5 mm of core (to minimize contamination of the surface of the core), and placed in 17.7 x 19.5 cm Ziploc® freezer bags within 26.8 x 27.3 cm Ziploc® freezer bags (to minimize vapour loss). Samples were stored in coolers to maintain moisture and temperature stability until analyses of isotopes of water could be performed.

Core samples (7.5 cm in diam. x 10-20 cm long) were also collected every 3 m (where core recovery permitted) for determination of total porosity $n_t$ (n = 110) and analysis of extractable Cl concentrations (n = 93). Additional core samples (7.5 cm in diam. x 10-20 cm long) (two samples from the glacial till at 399 and 372 m asl and six from the Lower Colorado and KDF at 326, 314, 296, 281, 271,

and 261.6 m asl) were collected from corehole 140-10-087 for mechanical squeezing and subsequent measurement of the Cl concentrations. These core samples were wrapped in plastic wrap and masking tape and coated in paraffin wax in the field, before being stored in coolers to maintain moisture and temperature stability until tested.

Water samples were also collected from a 22-day pump test conducted in well 140-10-089 (75 m north and 69 m west of 140-10-087; October 25 to November 14, 2010; Figure 1). The well intake zone (3 mm stainless steel Johnson Screen) extended from 253.5 to 163 m asl, intersecting the Mannville aquifer from 191 to 163 m asl. The pumping rate was 0.056 $m^3 s^{-1}$. Three water samples were collected from the discharging groundwater. The first was collected on October 25, 2010 after $7.6 \cdot 10^2$ $m^3$ of water was pumped, the second on October 26, 2010 after $7.3 \cdot 10^3$ $m^3$, and the last on November 9, 2010 after $7.2 \cdot 10^4$ $m^3$. These samples were stored in 100 mL HDPE bottles at room temperature for stable isotope and Cl analyses. An additional water sample was collected from the pumping well on the final sampling date for $^{14}C_{DIC}$ analysis at room temperature in 250 mL HDPE bottles. Sample collection was performed in accordance with the national groundwater sampling protocol being developed by GNS Science in collaboration with the Ministry for the Environment, Greater Wellington Regional Council and Environment Canterbury (GNS Science 2010). This sample was submitted to Beta Analytic in Miami, Florida, for $^{14}C_{DIC}$ and $\delta^{13}C$ (‰) analyses.

*3.2 Sample Preparation*

3.2.1 Total Porosity

The total porosity ($n_t$) was calculated from bulk density ($\rho$) and gravimetric water content ($\omega$) measurements made on the core samples collected every 3 m in both coreholes (n=110). Determination of $\omega$ was conducted using the method outlined in ASTM D2216-10 (ASTM 2010). Determination of $\rho$, as well as the calculation of $n_t$, was performed in accordance with ASTM D7263-09 (ASTM 2009).

3.2.2 Squeezing of Porewater from Core Samples

The core samples from 140-10-087 were squeezed in a high-pressure mechanical squeezer using a method similar to Patterson et al. (1978) to obtain porewater samples for Cl analyses. Samples

were chipped and immediately packed into the squeeze cylinder (316 L stainless steel; 50 mm diam. x 80 mm long). The piston was inserted into the cylinder, placed in a hydraulic press, and the pressure increased to 50 MPa and maintained for 3-5 days. This pressure was selected because testing by Bangsund et al. (in prep) showed no measurable effects on the pore-water Cl concentration at this pressure. The porewater passed through a 0.45 µm stainless steel filter before exiting the squeezer through a port located at the base of the cylinder, where it was collected in a clean 60-$cm^3$ syringe and transferred to a 20 mL scintillation vial, where it was stored at room temperature for analysis.

3.2.3 Aqueous Extractions from Core Samples for Cl Analyses

Core samples were dried in an oven for 48 hours at 90°C and pulverized using a titanium carbide swing mill. To determine the optimum leaching time and water: rock ratio for aqueous extraction of Cl, batch testing was performed on three samples (from 305, 290, and 249 m asl) from OVB-10-207. Based on leaching times of 1, 5, 10, and 100 hours and water: rock ratios of 2:1, 3:1, 4:1, and 5:1 (data not presented), an optimum extraction technique was devised, where 10 g of ground core sample was mixed with 20 mL of nanopure water, then shaken with a Burrell Scientific Model 75 wrist action shaker, centrifuged at 3000 rpm for 2 hours in an IEC Centra-4B centrifuge, and filtered through 0.45 µm nitrate membrane filter paper (Schmeling 2012). The resulting aqueous phases were collected in 20 mL scintillation vials and stored at room temperature for Cl analyses.

Porewater Cl concentrations were determined for core samples using the aqueous extract data and a method similar to van Loon et al. (2007). In the technique used the core samples were dried in an oven at 90°C for 48 h, powdered using a titanium carbide swing mill, and the Cl extracted using a 3:1 DI water:solid ratio for 1 h. Testing showed the water:solid ratio and time of extraction effectively removed the soluble Cl from the solid core samples (Schmeling 2013). The porewater Cl concentration for each extract sample ($C_{pw}$; n=94) was calculated from the analyte Cl concentration using:

$$C_{pw} = C_R \cdot \rho \cdot \frac{V_L}{M_R} \cdot \frac{1}{n_e}, \quad [1]$$

where $C_R$ is the mass of Cl per volume of pore fluid (mg $L^{-1}$), $M_R$ is the mass of solute per mass of bulk sample, $\rho$ is the bulk density, $V_L$ is the volume of leach solution per mass of bulk sample

leached (the water to rock ratio used in the extraction) and $n_e$ is the effective porosity (Waber and Smellie 2008). Mazurek et al. (2011) and Koroleva et al. (2011) compare anion concentrations from aqueous leaching tests to squeezed waters from the same rocks to determine the $n_e$ in equation [1]. The $n_e$ of the Saskatoon Group till and Lower Colorado shale were estimated by multiplying the $n_t$ (calculated from ρ and ω) by the ratio of anion to water accessible porosity, such that the extracted Cl concentrations matched the limited squeezed Cl concentrations. To determine the $n_e$ of the Lower Mannville, the Mannville groundwater samples collected during the pump test were used to approximate the porewater Cl concentration.

*3.4 Sample Analysis*

The $\delta^2H$ and $\delta^{18}O$ of the porewater in core samples (n=303) were determined using $H_2O_{(liquid)}$-$H_2O_{(vapour)}$ porewater equilibration and laser spectroscopy on a Picarro cavity ringdown spectrometer LII02-i (Wassenaar et al. 2008). The medium sized Ziploc™ bags containing the core samples were inflated with $H_2O$-free dry air and resealed. The samples were then replaced in the large Ziploc™ bag they were stored in and the air removed. The samples were allowed to equilibrate at room temperature to 100% for 3 days prior to analysis. To correct for instrumental drift and to normalize the results to the VSMOW scale two water standards with $\delta^{18}O$ and $\delta^2H$ values that bracketed that of the porewaters in the core samples were prepared and run after every four samples. The accuracy and precision of this method is better than ±0.3‰ for $\delta^{18}O$ and ±0.8‰ for $\delta^2H$ relative to the Vienna Standard Mean Ocean Water (VSMOW) reference (Hendry et al. 2011; Wassenaar et al. 2008). By spiking the drill mud with 99% $D_2O$ to values of $\delta^2H$ up to -30‰ at 140-10-087 and OVB-10-207, contamination of the core subsamples by drilling fluid was determined. Drill mud samples were collected every six hours during coring for analyses of $\delta^2H$ and $\delta^{18}O$. These values were compared to measured values from the core samples to evaluate contamination in the core samples (Hendry et al, 2012). Spiked drill fluids, as well as water samples collected from the pumping well were analyzed for $\delta^2H$ and $\delta^{18}O$ using a Los Gatos liquid isotope analyzer, with accuracies of ± 0.8‰ for $\delta^2H$ and ± 0.1‰ for $\delta^{18}O$ (Lis et al. 2008) relative to VSMOW. Chloride analyses were performed on the samples from the mechanically squeezed porewaters, the

pump discharge samples and the core extract samples using a Dionex IC25 ion chromatograph (IC) and AS50 autosampler with an accuracy and precision of <5% and a detection limit of 1.0 mg $L^{-1}$.

The water sample from the pumping well for $^{14}C_{DIC}$ and $\delta^{13}C$ (‰) analyses was analyzed by reducing the sample carbon to graphite (100% C), which was in turn analyzed for $^{14}C_{DIC}$ in an accelerated mass spectrometer (AMS). The $^{14}C_{DIC}$ content was reported as fraction of modern day carbon (Fmdn) with an accuracy of ±0.0008. The corrected age of the DIC was calculated using NETPATH geochemical modeling software (Plummer et al. 1994) using a method of El-Kadi et al. (2011a,b). NETPATH applies the traditional correction models including those of Tamers (1975), Ingerson and Pearson (1964), Mook (1972), Eichinger (1983), and Fontes and Garnier (1979).

## 4.0 Results and Discussion

### *4.1 Geology of Coreholes*

The geology and unit thicknesses at 140-10-087 and OVB-10-207 were defined from the geologic core logs (Figure 2). Borehole 140-10-087 was drilled to 93 m asl. It intersected Holocene-aged surficial sands and silt (445.6 to 441 m asl); Pleistocene aged Saskatoon (441 to 339 m asl) and Sutherland Group (339 to 327 m asl) glacial sediments; Late-Cretaceous aged Lower Colorado shale (327 to 251 m asl); Mannville group sand, silt, and shale (251 to 99 m asl); and Souris River dolomite (99 to 93 m asl). Kimberlite was observed within the Lower Colorado shale (KDF between 313 and 281 m asl and Pense volcaniclastic kimberlite (PVK) between 257 and 251 m asl) (Figure 2). Borehole OVB-10-207 was drilled to 239 m asl. It intersected Holocene-aged surficial sand and lacustrine clay (443 to 404 m asl); Pleistocene-aged Saskatoon (404 to 335 m asl) and Sutherland Group (335 to 330 m asl) till; Late-Cretaceous aged Lower Colorado shale (330 to 246 m asl); and Mannville sand, silt, and shale (246 to 239 m asl) (Figure 2). Overburden distribution and thicknesses are in keeping with findings of Christiansen and Sauer (1993). The location of Lower Colorado and Mannville Group sediments as well as the distribution of kimberlite is in keeping with Zonneveld et al. (2004), Berryman et al. (2004), and Kjarsgaard et al. (2007, 2009).

### *4.2 Total Porosity*

At both boreholes, the $n_t$ of the Saskatoon (140-10-087: 0.15±0.07, n=15; OVB-10-207: 0.17±0.03 n=13) and Sutherland Group tills (140-10-087: 0.25±0.05, n=4; no samples collected at OVB-10-207) were uniform with depth (Figure 3). The $n_t$ of the Lower Colorado shale was uniform with depth at OVB-10-207 (0.34±0.04, n=26) and 140-10-087 (0.34±0.03, n=10); however, the emplacement of KDF (313 to 281 m asl) in 140-10-087 disturbed the shale in this borehole, resulting in a greater standard deviation within this zone (0.33±0.09, n=8; Figure 3). Where the Lower Colorado shale was not disturbed by kimberlite (OVB-10-207), $n_t$ values decreased with depth from 0.38 at 330 m asl to 0.31 at 248 m asl, consistent with findings of Shaw and Hendry (1998) and Hendry et al. (2011) for shale of the Snakebite member of the Bearpaw Fm, 25 Ma younger than the shale at the current study site and Smith et al (2012) for the Pierre, 1st and 2nd White Speckled and Belle Fourche shales.

*4.3 $\delta^2H$ and $\delta^{18}O$ Profiles*

Porewater $\delta^2H$ and $\delta^{18}O$ values for all core samples at 140-10-087 and OVB-10-207, as well as Mannville groundwater collected during the pump test were cross plotted in Figure 4. The $\delta^2H$ and $\delta^{18}O$ values of the three Mannville groundwater samples collected during the pump test lie on the LMWL and ranged from -143 to -145‰ and -18.3 to -18.6‰, respectively (Figure 4). The data sets for 140-10-087 and OVB-10-207 yielded linear trends ($\delta^2H = 5.87\ \delta^{18}O$-52.12, $R^2 = 0.82$ and $\delta^2H = 6.50\ \delta^{18}O$-27.45, $R^2 = 0.80$, respectively). The shallow slope of the lines with respect to the local meteoric water line for Saskatoon (LMWL; $\delta^2H = 7.73\ \delta^{18}O$-1.72, $R^2 = 0.96$; Hendry et al. 2011) suggests the core samples may have been impacted by evaporation after sampling (Hendry et al. 2011; Kelln et al. 2001). The $\delta^2H$ and $\delta^{18}O$ values of the rotary drill fluid spiked during coring for each corehole plot above the LMWL with $\delta^2H$ and $\delta^{18}O$ values ranging from -28 to -150‰ and from -14 to -19‰ at 140-10-087 and from -48 to -111‰ and from -15 to -16‰ at OVB-10-207 (Figure 4; Hendry et al. 2012). The few core samples from each corehole that plot above the LMWL (n=18) are consistent with the values for the spiked drill fluids. As such, these values were considered contaminated and not discussed further.

Pore-water $\delta^2H$ vs. $\delta^{18}O$ were plotted for all core samples collected from both drillholes, as well as Mannville groundwater collected during the pump test (Figure 4). Core samples collected from the glacial till range from -138 and -15‰ to -171 and -19‰ for $\delta^2H$ and $\delta^{18}O$, respectively, ranging from

283 modern meteoric water at the surface to glaciogenic water at the base of the glacial till. Core samples
284 collected from the Lower Colorado and Upper Mannville are isotopically different than core samples
285 collected from the lower Mannville. Lower Colorado and upper Mannville core samples range from -168
286 and -19‰ to -147 and -16‰ for $\delta^2H$ and $\delta^{18}O$, respectively, reflecting a glaciogenic origin of the
287 porewater (Hendry and Wassenaar 1999; Remenda et al. 1996). Core samples collected from the lower
288 Mannville range from -132 and -15‰ to -151 and -16‰ for $\delta^2H$ and $\delta^{18}O$ and suggest the presence of
289 meteoric waters (-132 and -15‰; Figure 4). Because $\delta^2H$ and $\delta^{18}O$ are linearly correlated, $\delta^2H$ was used
290 to describe the transport of the stable isotopes of water at the Shore Gold study site. The $\delta^2H$ vapour
291 values at 140-10-087 are presented in Figure 5a. These data showed a well-defined trend with depth
292 from ground surface, through the glacial till, Lower Colorado shale, upper and lower Mannville. The $\delta^2H$
293 values decrease from -137‰ at 45 m BG to -171‰ at the contact between the glacial till and shale
294 contact (327 m asl). The $\delta^2H$ values then remain vertically constant from 327 m asl to the base of the
295 fractured zone at 301 m asl (Schmeling et al. in review). Below the fractured zone the vapour $\delta^2H$ values
296 increase from -171‰ to -147‰ in the Lower Colorado shale (between 301 and 251 m asl) and decrease
297 again from -147‰ at the contact between the Lower Colorado and Upper Mannville to -171‰ in the
298 middle of the upper Mannville (211 m asl). Vapour $\delta^2H$ values increase again from -171‰ at 311 m asl to
299 -145‰ at the contact between the upper and lower Mannville, where the $\delta^2H$ trend with depth remains
300 vertically constant to the contact between the lower Mannville and the Souris River dolomite (99 m asl;
301 Figure 5a). The vertically constant trends observed between 327 and 300.6 m asl in the fractured zone
302 and between 191 to 99 m asl in the lower Mannville aquifer were similar to vertical trends in tracer profiles
303 that have been observed by Hendry and Wassenaar (2004) in the Quaternary till and Pierre shale at the
304 Lanigan site and Kelln et al. (2001) in Battleford and Floral till and have been identified as zones
305 dominated by advective transport. The pump test water $\delta^2H$ values are consistent with values determined
306 on Lower Mannville core samples at 140-10-087 (Figure 5a) and suggest the dominant source of pump
307 test water was the Lower Mannville aquifer, located 191 to 99 m asl. The small range in $\delta^2H$ and $\delta^{18}O$
308 values of the three samples with time (and volume pumped) also suggests no measurable vertical
309 leakage from the overlying Upper Mannville or Lower Colorado shale during pump testing; a decrease in
310 $\delta^2H$ and $\delta^{18}O$ values would have been observed had vertical leakage occurred.

The $\delta^2H$ depth-trend at OVB-10-207 (Figure 5b) was less complex than the data from 140-10-087. For example, unlike the $\delta^2H$ trend in the glacial sediments at 140-10-087, the $\delta^2H$ trend in the glacial sediments at OVB-10-207 was vertically constant with depth (33 to 90 m BG) and ranged from -127 to -141‰. This trend suggested that the transport process through this unit may be dominated by advection. A curvilinear trend was also observed in the Lower Colorado, ranging from -156‰ at the top and increasing with depth to -144‰ at the top of the Upper Mannville. The gap in the $\delta^2H$ profile between 90 and 125 m prevented comment on the dominant transport mechanisms or pore-water age and origin in this zone. The curvilinear Cl concentration profile over the same depth (discussed below) suggested the $\delta^2H$ trend of this profile, between the base of the intertill aquifer (326 m asl) and the top of the Mannville aquifer (248 m asl), was also curvilinear and diffusion was the dominant transport mechanism.

*4.4 Anion Accessible Porosity and Chloride Profiles*

The $n_e$ for Cl was constrained by comparing Cl concentrations obtained by aqueous leaching with porewater Cl concentrations from mechanical squeezing and from Mannville groundwater samples collected during the 22 day pump test (Koroleva et al. 2011). The calculated $n_e$ values in the glacial till using this method were determined to range from 0.13 to 0.16 and the percentage of $n_e$ to $n_t$ was determined to be 100%, indicating that all of the connected pore space was accessible to anions. The ratio of $n_e$ to $n_t$ was also 100% in the upper part of the Lower Colorado (327 to 313 m asl) and in the KDF (313 to 291 m asl). The ratio of $n_e$ to $n_t$ was 45% in the Lower Colorado and Pense kimberlite, resulting in $n_e$ values ranging from 0.19 to 0.14. This ratio suggests that only 45% of the connected pore space in this media was accessible to anions. Using the Mannville groundwater from the 22 day pump test as a comparison, the Upper Mannville shale, silt, and sand Cl data yielded a ratio of $n_e=0.45n_t$, resulting in $n_e$ values ranging from 0.09 to 0.17. Similarly, the Lower Mannville sand Cl concentrations from aqueous leaching yielded a ratio of $n_e=0.6n_t$, with $n_e$ values ranging in this unit from 0.11 to 0.20. The Lower Colorado shale and KDF in 140-10-087 yielded $n_e$ values equal to those estimated in the glacial till. This could be due in part to the considerably lower clay fraction within the KDF (313 to 291 m asl), which ranged from 9.9 to 15.2 wt%, whereas the shale below the KDF yielded clay contents in the range of 47.3 to 64.7 wt% (Schmeling in prep). The presence of fractures between 327 and 291 m asl (Schmeling, in

prep) could also contribute to this high effective porosity in the Lower Colorado unit. Additional work is required in kimberlite media to explain the presence of these high $n_e$ values. Similar ratios of $n_e$ to $n_t$ have been widely reported in clay rich aquitard units. Mazurek et al. (2011) report ratios of $n_e$ to $n_t$ of 0.43 in the Boom Clay in Belgium and 0.5 in the Callovo-Oxfordian Clay in France. Similarly, Hendry et al. (2000) report ratios of 0.3 in the Battleford till and 0.38 in the snakebite clay in Saskatchewan, Canada.

XRD and clay content analysis of Lower Colorado shale core samples indicate the mineralogy and clay content of the Lower Colorado shale (not including KDF) in both 140-10-087 and OVB-10-207 are similar (Schmeling in prep). As such, the $n_e$ calculated at 140-10-087 (0.45) was applied to the Cl concentrations of core samples from aqueous leaching in the Lower Colorado shale at OVB-10-207.

The vertical distribution of calculated porewater Cl concentrations [equation 1] with depth at 140-10-087 and OVB-10-207 are presented in Figure 7. At 140-10-087, the Cl concentrations in the glacial till (399 to 327 m asl) and fractured Lower Colorado and KDF (327 to 291 m asl) are vertically constant and range from 230 to 820 mg $L^{-1}$. The uniform distribution of Cl in the fractured Lower Colorado and KDF at borehole 140-10-087 may be attributed to advection through the fractures, resulting in a constant concentration through the zone. Below the fractured zone in the Lower Colorado shale and KDF (291 m asl) the pore-water Cl concentration increases from 980 mg $L^{-1}$ to 3500 mg $L^{-1}$ at the boundary between the Lower Colorado and Upper Mannville (247 m asl), then decreases again to 1200 mg $L^{-1}$ at 225 m asl. Below 225 m asl the concentration remains vertically constant, ranging from 1200 to 3500 mg $L^{-1}$ with an average of 2100 mg $L^{-1}$ to the base of the Mannville at 99 m asl.

At OVB-10-207 the lack of variability in Cl concentration with depth in the glacial till, like that observed at 140-10-087, was attributed to homogenization of the till during deposition, which resulted in an initially uniform vertical Cl profile through the till (Hendry et al. 2000). The Cl concentration in the glacial till ranged from 140 to 450 mg $L^{-1}$ with depth (410 to 330 m asl; Figure 7b). A symmetrical, well-defined diffusion trend was observed in the Lower Colorado shale, between the base of the glacial till (330 m asl) and the top of the Upper Mannville (248 m asl), increasing from 1200 mg $L^{-1}$ at the top of the Lower Colorado shale (329 m asl) to 4300 mg $L^{-1}$ in the middle of the Lower Colorado (284 m asl), then decreasing with depth again to 1400 mg $L^{-1}$ at the top of the Upper Mannville (248 m asl).

### *4.5 $^{14}C_{DIC}$ Age Dating of a Mannville Water Sample*

The apparent $^{14}C_{DIC}$ age of the pump test Mannville groundwater sample was estimated to be 22330±100 a BP, as calculated from the fraction of modern (Fmdn) of 0.0621±0.0008 and a $\delta^{13}C$ value of -12‰. The corrected radiocarbon age of the Mannville groundwater was estimated to be between 15,700 and 22,000±100 a BP. Table 1 presents a summary of ages of the Mannville groundwater determined using these traditional adjustment models. These results are consistent with the Mannville Group water being recharged by an influx of glaciogenic water during the Pleistocene. Grasby and Betcher (2000) suggest low $\delta^{18}O$ (and $\delta^{2}H$) values of formation waters, collapse structures related to salt dissolution, hydrodynamic blowout structures, and biodegradation of oils all imply a significant influx of fresh water into the Williston Basin along the outcrop belt in southern and central Manitoba during Pleistocene glaciation. The thickness of the continental ice sheet during the Pleistocene could have provided sufficient hydraulic head to reverse the hydraulic gradient and flow direction within the Williston Basin. Grasby et al. (2000) suggest a considerable influx of fresh water up to ~300 km beyond the outcrop limit in Manitoba as a result of this Pleistocene flow reversal. More local injection of meltwater may have occurred through collapse features (Wittrup and Kyser, 1990) or as inflow from the Saskatchewan river.

### *4.6 Defining Initial and Boundary Conditions for Transport Modeling of $\delta^{2}H$ and Cl in the Cretaceous*

Transport modeling of 1-D vertical tracer profiles ($\delta^{2}H$ and Cl) require knowledge of the timing and initial conditions for the tracer profiles. This infromantion can be estimated from geologic and hydrogeological history of the region. The gap in $\delta^{2}H$ data between 368 and 318 m asl at OVB-10-207 compromised the usefulness of this profile for determining the hydrogeologic evolution of the study area, as well as for transport modeling. Fortunately, no such gap was present in the pore-water Cl data. Similarly, the poorly defined boundary conditions in the pore-water Cl concentration profile with depth at 140-10-087 compromised the usefulness of this profile for determining the hydrogeologic evolution and transport modeling. Because the $\delta^{2}H$ profile at 140-10-087 was more completely defined than that at OVB-10-207 (i.e., it included glacial till and the upper and lower Mannville profile), it was considered the most useful for defining the hydrogeological evolution of the study area, and as such, the initial and boundary conditions for transport modeling. As such the $\delta^{2}H$ profile at 140-10-087 was modeled first to

define the timing of evolution of the $\delta^2H$ profile through the shale. This evolution timing would later be applied to the Cl concentration profile with depth at OVB-10-207.

4.6.1 Hydrogeological Evolution of the Study Area and the Impact on Initial and Boundary Conditions for the Tracers

Based on the hydrogeologic history of the region, the $\delta^2H$ profile at 140-10-087 and the pore-water Cl concentration profile at OVB-10-207 were hypothesized to be the result of the following sequences of events. The Upper and Lower Mannville shale, silt, and sand were deposited between 104-112 Ma BP in a terrestrial environment, which transitioned into a marine setting when the Lower Colorado shale was deposited, between 99 and 104 Ma BP (Zonneveld et al. 2004). Because the shale was deposited by an epi-continental sea, which covered North America during the Cretaceous, a $\delta^2H$ value and Cl concentration of seawater (0‰ and 21,000 mg $L^{-1}$) were assumed for the initial concentration of the porewater in the shale at the time the boundary conditions changed, at the onset of the Pleistocene (Mazurek et al. 2011). Two important events occurred during the Pleistocene: (1) the deposition of the Sutherland group (0.5 to 2.5 Ma BP) and Saskatoon Group (38-500 Ka BP) glacial sediments (Christiansen 1968; Christiansen and Sauer 1993), which changed the boundary condition on the top of the Lower Colorado to reflect a glacial signature that has been modified by transport of -171‰ that existed throughout the deposition of the Saskatoon and Sutherland group tills (Hendry and Wassenaar 1999; Hendry et al. 2011; Remenda et al. 1996), and (2) the pore-water of the upper and lower Mannville that had a glacial signature, also modified by transport, of -169‰ was recharged by an influx of glaciogenic water due to flow reversal in the Williston Basin (Grasby and Betcher 2000) up to ~300 km from the outcrop area in Manitoba (Grasby et al. 2000). Lower Mannville groundwater had an isotopic signature between glaciogenic water, influenced by transport (-169‰) and modern water (-138‰; (Hendry and Wassenaar 1999) with an average value of -145‰. This was taken to be an influx of non-glaciogenic water after the Pleistocene from the outcrop area in Manitoba. Following the Pleistocene, the Holocene period (9.5-12 ka BP) was marked by deposition of surficial sand and lacustrine clay at the study site up to 55 m thick (Christiansen and Sauer 1993). The warming trend of the Holocene was

418 recorded by a shift to modern $\delta^2H$ values of -138‰ at 140-10-087 (Hendry and Wassenaar 1999; Hendry
419 et al. 2011).

420 *4.7 Characterizing the Evolution of the $\delta^2H$ and Cl at 140-10-087 and OVB-10-207 after Activation of the*
421 *Mannville and Glacial Intertill Aquifers*

422 The 1-D advective-diffusive transport of a conservative tracer ($\delta^2H$ and Cl) through an aquitard
423 system can be described by the partial differential equation:

424 $$\frac{\delta}{\delta t}(nC) = nDe\frac{\delta^2 C}{\delta x^2} - nV\frac{\delta C}{\delta z}, \quad [2]$$

425 where $D_e$ is the effective diffusion coefficient, V is the average linear velocity, C is the mass
426 concentration of the solute, z is the distance, and t is the time. In [2], $D_e$ is defined according to Fick's first
427 law as:

428 $$J_d = -n_e D_e \frac{\delta C}{\delta z}, \quad [3]$$

429 where is the diffusive mass flux rate and is the effective porosity. When considering $\delta^2H$, $n_e=n_t$; when
430 considering Cl at this study area $n_e=0.45n_t$ (Hendry and Wassenaar 1999; Hendry et al. 2011). The finite
431 element model SEEP/W was coupled with CTRAN (GEO-SLOPE International Ltd. 2007) to simulate the
432 $\delta^2H$ and Cl profiles with time using equation [2]. Because $\delta^2H$ profile at 140-10-087 was more well
433 defined than that for the Cl profile at OVB-10-207 the $\delta^2H$ profile with depth (401 to 186 m asl) at 140-10-
434 087 was modelled first followed by the simpler Cl profile (313 to 251 m asl) at OVB-10-207. The presence
435 of the Holocene warming period (10 ka) and the $^{14}C_{DIC}$ age date of the Mannville Groundwater (15-22 Ka)
436 at 140-10-087 also provided useful time constraints for calibration.

437 4.7.1 Characterizing the Evolution of $\delta^2H$ at 140-10-087

438 Because the upper and lower boundary conditions in the pore-water Cl concentration profile with depth at
439 140-10-087 could not be defined, only the $\delta^2H$ profile was considered for transport modeling at this
440 corehole. The 1-D vertical model for $\delta^2H$ transport at 140-10-087 was constructed as a column of
441 elements (1 m wide) with 74 m of glacial till, 76 m of Lower Colorado and related kimberlite deposits (KDF

and PVK), 60 m of upper Mannville shale, silt, and sand, and 95 m of lower Mannville sand. Initially, the curve in the Lower Colorado and upper Mannville (301 to 191 m asl) was modeled to determine the best fit (determined visually) to the measured profile with depth. Subsequently, a second advection-diffusion analysis was conducted to determine the best fit to the upper-lower Mannville profile with depth (216 to 196 m asl) and then a third advection-diffusion analysis was modeled to determine the best fit to the measured profile in the glacial till (401 to 327 m asl). Each subsequent analysis was modeled using the best fit parameters estimated from the previous analysis, and the results of the most recent time step of each previous analysis for the initial conditions.

The upper boundary condition in the first advection-diffusion analysis for $\delta^2H$ at 140-10-087 was defined as the base of the fractured zone in the Lower Colorado (301 m asl) and assigned a value of -170‰. The lower boundary condition was defined as the base of the Upper Mannville (191 m asl) and assigned a constant value of -185‰. In the second analysis, the bottom boundary condition was assigned a value of -144‰ and run for 10, 15 and 20 ka to match the observed mixing trend between the upper and lower Mannville. The initial value in the Lower Colorado and Upper Mannville sediments was defined as 0‰ (Cretaceous seawater). The model was assigned a porosity value of 0.25 in the glacial till, 0.34 in the Lower Colorado and 0.27 in the Mannville. The glacial till was assigned a $D_e$ of $6.0 \cdot 10^{-10}$ $m^2$ $s^{-1}$, consistent with high $D_e$ values in the sandy shale unit in the Boom clay in Belgium and the Callovo-Oxfordian clay, France (Mazurek et al. 2011), the Lower Colorado and upper Mannville shales were assigned a value of $2.3 \cdot 10^{-10}$ $m^2$ $s^{-1}$, consistent with Cretaceous shales in the Williston Basin (Hendry and Wassenaar 1999; Hendry et al, in review). The best fits (determined visually) to the measured $\delta^2H$ profile with depth occurred between 390 and 370 ka and an activation of the Mannville aquifer between 10 and 15 ka (Figure 7). The later is consistent with deposition of the Sutherland group till in the region (Christiansen 1968; Christiansen and Sauer 1993) and the $^{14}C_{DIC}$ age date of pump test water (Figure 9a). To lower the $\delta^2H$ value in the upper-lower Mannville curve (216 to 191 m asl), values lower than -180‰ were assigned to the lower boundary condition; however, glaciogenic water $\delta^2H$ values lower than -180‰ have not been reported in North America (Hendry and Wassenaar 1999; Hendry et al. 2011; Remenda et al. 1996). To fit the mixing curve in the glacial till to the measured $\delta^2H$ profile, the third advection-diffusion analysis was added to the model to simulate the mixing trend from the top of the

Lower Colorado fractured zone (where the $\delta^2H$ of the fractures and shale matrix are homogenized) at 327 m asl and the base of the surficial sand aquifer (401 m asl). The lower boundary condition was assigned to the fractured zone (327 to 301 m asl) and given a constant value of -170‰; the upper boundary condition was defined at 401 m asl and assigned a constant concentration of -136‰. The initial concentration in the till was assigned a value of -170‰. This analysis was run for the last 10 ka of the simulation to reproduce the transition into the Holocene. A base case was run as diffusion only with a $D_e$ of $6.0 \cdot 10^{-10}$ $m^2$ $s^{-1}$ that resulted in very poor fits to the measured data. Downward advective velocities were added to the simulation to assess the impact of a range in velocities on the modelled fit to the measured data. The model was run using downward advective velocities of 10, 12.5 and 15 m 10 $ka^{-1}$ (Figure 7). The best fit to the measured data was observed for an advective velocity of 12.5 m 10 $ka^{-1}$ at an evolution time of 10 ka, consistent with the timing of the Holocene and deposition of surficial sand and lacustrine clay in the study area (Christiansen and Sauer 1993). Because the pore-water Cl concentration profile at OVB-10-207 was initially vertically constant with depth, possibly due to homogenization during deposition (Hendry et al. 2000), these data could not be used to estimate timing of evolution or transport mechanisms at this corehole.

### 4.7.2 Effects of Velocity on the Evolution of $\delta^2H$ at 140-10-087

Additional simulations were undertaken to assess the impact of both vertical upward and downward advective velocities at 140-10-087 on the $\delta^2H$ profile in the Lower Colorado and upper Mannville shales (Figure 8). The simulated profile using an evolution time of 380 ka in the shale was the best fit to the measured data and was used to estimate the limit of vertical upward and downward advective. The curve in the glacial till was modeled using a $D_e$ of $6.0 \cdot 10^{-10}$ $m^2$ $s^{-1}$, a vertical downward advective velocity of 12.5 m 10 $ka^{-1}$, and an evolution time of 10 ka to represent the Holocene. Vertical upward and downward advective velocities of 0, 0.25, 0.50, and 0.75 m 10 $ka^{-1}$ were simulated in the Lower Colorado and upper Mannville. Again, consideration of diffusion only (V= 0 m 10 $ka^{-1}$) best described the shape of the measured $\delta^2H$ profile with depth in the Lower Colorado and upper Mannville shale at this site. The upper limit on vertical advective velocity was estimated at 0.5 m 10 $ka^{-1}$, both upward and downward, corresponding to a $K_v$ of $8 \cdot 10^{-12}$ m $s^{-1}$ (Figure 8), and an activation time in the

497 Mannville aquifer between 15 and 20 ka when considering upward vertical velocity and 10 ka, consistent
498 with the timing of the Holocene in the study area, when considering downward velocity. However,
499 advection dominates the zones of the $\delta^2H$ profile that are vertically constant, such as the fractured Lower
500 Colorado shale and KDF between 327 and 301 m asl and the Lower Mannville aquifer between 321 and
501 99 m asl.

502 4.7.3 Characterizing the Evolution of Cl at OVB-10-207

503 The $\delta^2H$ profile at OVB-10-207 could not be used for numerical transport modeling because of
504 the gap in data between 368 and 318 m asl. Fortunately, however, no such gap existed in the Cl data.
505 The curved mixing trend at OVB-10-207 begins at the boundary between the glacial till and Lower
506 Colorado shale (Figure 7b), with a curved, approximately symmetrical profile existing throughout the
507 Lower Colorado shale. Cl values decrease toward the aquifers both above and below (Saskatoon intertill
508 and upper Mannville), suggesting that the Mannville sediments at this site do not exhibit the same low K
509 directly below the Lower Colorado, as observed at 140-10-087, but rather represent a permeable zone
510 directly at the base of the Lower Colorado. The Cl concentration of Mannville Group sediments at OVB-
511 10-207 (1400 mg $L^{-1}$) also suggests this may be the case, because the top of the Mannville at 140-10-087
512 exhibits high Cl concentrations similar to the Lower Colorado (Figure 6a, b). Moreover, the curved,
513 symmetrical profile of $\delta^2H$ in 140-10-087 extended 50 m into the Mannville sediments, a trend not
514 observed in the Cl profile with depth at OVB-10-207 (Figure 5a, b).

515 A 1-D vertical model was constructed as a column of elements (1 m wide) comprised of two
516 regions: 80 m of glacial till overlying 78 m of Lower Colorado shale. The near symmetrical shape of the
517 Cl concentration profile with depth between the two bounding aquifers suggests they were activated at
518 similar times (Figure 7). The glacial till displayed a vertically uniform profile, with the upper boundary
519 condition defined as the intersection of the glacial till and Lower Colorado shale and assigned a constant
520 value of 270 mg $L^{-1}$, which was the average value of pore-water Cl concentration in the till. The average
521 Cl concentration at the top of the Mannville Group aquifer was defined as the lower boundary condition
522 and assigned a constant concentration of 1,400 mg $L^{-1}$. The initial concentration of the shale was
523 assigned a value of 21, 000 mg $L^{-1}$, the assumed Cl concentration of seawater during the Cretaceous

when the shale was deposited. One advection-diffusion analysis was simulated using an $n_e$ value of 0.16 and a $D_e$ for the shale of $1.2 \cdot 10^{-10}$ $m^2$ $s^{-1}$, consistent with Cretaceous shale in the Williston Basin (Hendry et al 2000) and Ordivician shale in Ontario (Barone et al 1990). The best fit to the measured Cl profile with depth was observed between 390 and 370 ka (Figure 9a).

4.7.4 Effects of Velocity on the Evolution of the Cl at OVB-10-207

Alternate model simulations were run considering both upward and downward vertical advective velocities through the Lower Colorado at OVB-10-207 (Figure 9b, c). Upward and downward vertical advective velocities of 0.25, 0.50 and 0.75 m 10 $ka^{-1}$ were used in the model (Figure 9b, c). Diffusion alone best explained the observed, nearly symmetric Cl profile using hydrogeologically plausible parameters; however, the advective velocities where the model simulations no longer fit the observed Cl profile occurred at V values of >0.50 m 10 $ka^{-1}$ suggesting the upper limit of advective flow, both vertically upward and downward (Figure 11). This vertical velocity corresponds to a $K_v$ of $8 \cdot 10^{-12}$ m $s^{-1}$, consistent with the undisturbed Lower Colorado and upper Mannville shales at 140-10-087.

## 5.0 Summary and Conclusions

High-resolution profiles of the natural tracers $\delta^2H$ and Cl were collected at two drillholes at the Shore Gold study site in central Saskatchewan, Canada, to evaluate solute transport through Cretaceous shale. At one site the shale is highly fractured by kimberlite volcanism (140-10-087) whereas at the other site, the shale is minimally affected by kimberlite volcanism (OVB-10-207). A gap in $\delta^2H$ data at OVB-10-207 and uncertain initial and boundary conditions in the Cl profile at 140-10-087 limited transport modeling to the Cl profile at OVB-10-207 and the $\delta^2H$ profile at 140-10-087. These profiles show the value for applying multiple tracers to multiple drillholes.

The shape of the Cl profile at the site with no kimberlite (OVB-10-207) and associated vertical transport modeling show molecular diffusion to be the dominant vertical transport process through the Lower Colorado shale. The shape of the $\delta^2H$ profile with depth at the kimberlite affected site (140-10-087) suggests the presence of a permeable zone in the Lower Colorado shale and KDF between 327 and 301 m asl, and that advection is the dominant transport process in the Lower Colorado shale KDF

between 327 and 301 m asl. This advective zone is attributed to the emplacement of kimberlite (Schmeling 2013). The shape of the $\delta^2H$ profile at this site and associated vertical transport modeling suggest that the dominant transport process below this zone (301 to 190 m asl) is molecular diffusion, not only through the Lower Colorado shale but also 50 m into the Mannville formation, which is commonly considered to be an aquifer within the Williston Basin. This observation is consistent with the presence of laminated silts and clays, not the typical massive unconsolidated sandstone typical of the Mannville formation, in the upper 50 m of the Mannville formation at this corehole . The application of a range in vertical advective velocities across the Lower Colorado at both OVB-10-207 and 140-10-087 in the modeling exercises suggest that the upper limit of advective velocity is about 0.5 m 10 $ka^{-1}$ at both coreholes. Using measured hydraulic gradient data and this maximum velocity yielded a $K_v$ values at both drillholes of about $8 \cdot 10^{-12}$ m $s^{-1}$, where kimberlite is not observed. The evolution timings of both the $\delta^2H$ profile at 140-10-087 and the Cl profile at OVB-10-207 determined from the modeling exercise (390 to 370 ka using $D_e$ values of $2.3 \cdot 10^{-10}$ $m^2$ $s^{-1}$ and $1.2 \cdot 10^{-10}$ $m^2$ $s^{-1}$, respectively) are consistent with deposition of the Saskatoon and Sutherland Group till in the area. Modeling of the $\delta^2H$ profile at 140-10-087 also suggested that, the Mannville aquifer was recharged with glacial water during the Pleistocene, consistent with the findings of Grasby and Betcher (2000). It further suggested that a shift from glacial water to more modern water in the Mannville aquifer occurred in the last 10-20 ka BP. The simulated age is consistent with the $^{14}C_{DIC}$ date determined for a sample of Mannville groundwater collected during this study. Model simulations for the $\delta^2H$ profile collected at 140-10-087 also support the timing of the onset of the Holocene in the region at about 10 ka BP, consistent with other investigations in the area (Christiansen and Sauer 1993).

Studies using natural tracer profiles at geologically complex study sites are rare (see Introduction). This study shows that generating and interpreting natural $\delta^2H$ and Cl profiles in complex aquitard systems can improve our understanding of groundwater flow and solute transport mechanisms. In the case of the current study, these data improved our understanding of the impact of kimberlite volcanism on solute transport mechanisms of Lower Colorado and Upper Mannville shales. Despite a high degree of deformation in the region caused by kimberlite emplacement, solute transport mechanisms in the Lower Colorado shale (where no kimberlite was observed) is dominated by diffusion. This study

578 also showed that natural tracer profiles ($\delta^2H$ and Cl) can be used to estimate groundwater flow, solute
579 transport mechanisms, groundwater residence times, and the geologic history of complex, fractured
580 aquitard systems and provide a means of confirming hydraulic data collected at a given study site.

581 **Acknowledgements**

582 We are grateful to Ethan Richardson, Chad Wilkinson, and Terry Burkholder for field technical
583 support and data acquisition and L.I. Wassenaar, S. L. Barbour, V. Chostner, L. Smith, and F. Nelson for
584 their technical assistance. Financial support was provided by Shore Gold Inc. and the Natural Sciences
585 and Engineering Research Council of Canada through the Senior NSERC Industrial Research Chair
586 program (M.J.H.).

587 **References**

588 American Society for Testing and Materials (ASTM) (2009) D7263-09: Standard Test Methods for
589 Laboratory Determination of Density (Unit Weight) of Soil Specimens. In: Annual Book of ASTM
590 Standards, West Conshohocken, PA

591 American Society for Testing and Materials (ASTM) (2010) D2216-10: Standard Test Methods for
592 Laboratory Determination of Water (Moisture) Content of Soil and Rock by Mass. In: Annual Book
593 of ASTM Standards, West Conshohocken, PA

594 Bangsund AL, Hendry MJ (in prep) Geochemical effects of incremental high-pressure squeezing on pore
595 waters of consolidated and overconsolidated clays

596 Berryman AK, Scott-Smith BH, Jellicoe B (2004) Geology and diamond distribution of the 140/141
597 kimberlite, Fort á la Corne, central Saskatchewan, Canada. Lithos 76(1):99–144

598 Cey BD, Barbour SL, Hendry MJ (2001) Osmotic flow through a Cretaceous clay in southern
599 Saskatchewan, Canada. Can Geotech J. 38:1025–1033

600 Christiansen EA (1968) Pleistocene stratigraphy of the Saskatoon area, Saskatchewan, Canada. Can J
601 Earth Sci 5:1167–1173

602 Christiansen EA (1978) Geology of the Nipawin Dam Site (Axis No 5) Area and a Proposal for Additional
603 Studies. EA Christiansen Consulting Ltd. Saskatoon SK.

604 Christiansen EA, Sauer EK (1993) Red Deer Hill: a drumlinized glaciotectonic feature near Prince Albert,
605 Saskatchewan, Canada. Can J Earth Sci. 30:1224–1235

606 Clark JA (1982) Glacial loading: A cause of natural fracturing and a control of the present stress state in
607 regions of high Devonian shale gas production. In: SPE/DOE Unconventional Gas Recovery
608 Symposium of the Society of Petroleum Engineers, Pittsburg, PA 16–18 May 1982

609 Croisé J, Schlickenrieder L, Marschall P et al (2004) Hydrogeological investigations in a low permeability
610 claystone formation: the Mont Terri Rock Laboratory. Phys Chem Earth 29:3–15

611 Desaulniers DE, Cherry JA, Fritz P (1981) Origin, age and movement of pore water in argillaceous
612 Quaternary deposits at four sites in southwestern Ontario. J Hydrol 50:231–257

613 Eichinger L (1983) A contribution to the interpretation of $^{14}C$ groundwater ages considering the example
614 of a partially confined sandstone aquifer. Radiocarbon 25:347–356

615 El-Kadi AI, Plummer N, Aggarwal P (2011a) NETPATH-WIN: An interactive user version of the mass-
616 balance model, NETPATH. Groundwater 49(4):593–599

617 El-Kadi AI, Plummer N, Aggarwal P (2011b) Supporting information to: NETPATH-WIN: An interactive
618 user version of the mass-balance model, NETPATH. http://www-
619 naweb.iaea.org/napc/ih/documents/other/NETHPATH%20Supporting%20Info.pdf

620 Ewert WD, Brown FH, Puritch EJ et al (2009) Technical report and resource estimate update on the Star
621 Diamond Project, Fort á la Corne area, Saskatchewan, Canada. P&E Mining Consultants Inc.
622 Brampton, ON

623 Fontes JC, Garnier JM (1979) Determination of the initial $^{14}C$ activity of the total dissolved carbon: A
624 review of the existing models and a new approach. Water Resour Res 15:399–413

625 Gautschi A (2001) Hydrogeology of a fractured shale (Opalinus Clay): Implications for deep geological
626 disposal of radioactive wastes. Hydrogeol J 9:97–107

627 GEO-SLOPE International Ltd (2007) Seepage Modeling with SEEP/W 2007. An Engineering
628 Methodology 2nd Edition. Calgary AB

629 Gimmi T, Waber HN, Gautschi A et al (2007) Stable water isotopes in pore water of Jurassic argillaceous
630 rocks as tracers for solute transport over large spatial and temporal scales. Water Resour Res
631 43:W04410

632 GNS Science (2010) Sample Collection for Water Dating Analysis [online].
633 http://bullywug.gns.cri.nz/services/waterdating/cfc.html

634 Grasby SE, Betcher R (2000) Pleistocene recharge and flow reversal in the Williston basin, central North
635 America. J Geochem Explor 69–70:403–407

Grasby S, Osadetz K, Betcher R et al (2000) Reversal of the regional-scale flow system of the Williston Basin in response to Pleistocene glaciation. Geol 28(7):635–638

Hendry MJ, Wassenaar LI (1999) Implications of the distribution of δD in pore waters for groundwater flow and the timing of geologic events in a thick aquitard system. Water Resour Res 35(6):1751–1760

Hendry MJ, Wassenaar LI (2000) Controls on the distribution of major ions in pore waters of a thick surficial aquitard. Water Resour Res 36(2):503–513

Hendry MJ, Wassenaar LI, Kotzer T et al (2000) Chloride and chlorine isotopes ($^{36}$Cl and $\delta^{37}$Cl) as tracers of solute migration in a thick, clay-rich aquitard system. Water Resour Res 36(1):285–296

Hendry MJ, Kelln CJ, Wassenaar LI et al (2004) Characterizing the hydrogeology of a complex clay-rich aquitard system using detailed vertical profiles of the stable isotopes of water. J of Hydrogeol 293:47–56

Hendry MJ, Barbour SL, Zettl J et al (2011) Controls on the long-term downward transport of $\delta^{2}$H of water in a regionally extensive, two-layered aquitard system. Water Resour Res 47(W06505):1–13

Hendry, MJ, Wassenaar LI (2011) Millennial-scale diffusive migration of solutes in thick clay-rich aquitards: Evidence from multiple environmental tracers. Hydrogeol J 19:259–270

Ingerson E, Pearson FJ Jr (1964) Estimation of age and rate of motion of groundwater by the $^{14}$C-method, In: In: Recent Researches in the Fields of Atmosphere, Hydrosphere, and Nuclear Geochemistry. Sugawara Festival Volume. Ed. Y. Miyake and T. Koyama, 263-283, Maruzen Co., Tokyo

Kelln, CJ, Wassenaar LI, Hendry MJ (2001) Stable isotopes (δ18O, δ2H) of pore waters in clay-rich aquitards: A comparison and evaluation of measurement techniques. Ground Water Monit Remed 21(2):108–116

Kjarsgaard BA, Leckie DA, Zonneveld JP (2007) Discussion of “Geology and diamond distribution of the 140/141 kimberlite, Fort á la Corne, central Saskatchewan, Canada”, by A. Berryman, B.H. Scott-Smith and B.C. Jellicoe. Lithos 97:422–428

Kjarsgaard BA, Harvey S, McClintock M et al (2009) Geology of the Orion South kimberlite, Fort á la Corne, Canada. Lithos 112S:600 –617.

Koroleva M, Alt-Epping P, Mazurek M (2011) Large-scale tracer profiles in a deep claystone formation (Opalinus Clay at Mont Russelin, Switzerland): Implications for solute transport processes and transport properties of the rock. Chem Geol 280:284–296

Lefebvre N, Kurszlaukis S (2008) Contrasting eruption styles of the 147 Kimberlite, Fort á la Corne, Saskatchewan, Canada. J Volcanol Geotherm Res 174:171–185

Lis G, Wassenaar LI, Hendry MJ (2008) High-precision laser spectroscopy D/H and 18O/16O measurements of microliter natural water samples. Anal Chem 80(1):287–293

Mazurek M, Lanyon WG, Vomvoris S et al (1998) Derivation and application of a geologic dataset for flow modelling by discrete fracture networks in low-permeability argillaceous rocks. J of Contam Hydrol 35:1–17

Mazurek M, Alt-Epping P, Bath A et al (2009) Natural tracer profiles across argillaceous formations: The CLAYTRAC project. OECD/NEA Rep. 6253, OECD Nuclear Energy Agency, Paris, France

Mazurek M, Alt-Epping P, Bath A et al (2011) Natural tracer profiles across argillaceous formations. Appl Geochem 26(7):1035–1064

McNeil DH, Gilboy CF (2000) Cretaceous stratigraphy in four cores from the vicinity of the Fort á la Corne Kimberlite Field, east-central Saskatchewan-preliminary results. Saskatchewan Energy and Mines Miscellaneous Report 2000-4.1, Summary of Investigations 2000(1):98–105

Mook WG (1972) On the reconstruction of the initial $^{14}C$ content of groundwater from the chemical and isotopic composition. In: Proceedings of Eighth International Conference on Radiocarbon Dating, v. 1, Royal Society of New Zealand, Wellington, New Zealand: 342–352

Patriarche D, Ledoux E, Simon-Coinçon R et al (2004) Characterization and modeling of diffusion process for mass transport through the Tournemire argillites (Aveyron, France). Appl Clay Sci 26:109–122

Patterson RJ, Frape SK, Dykes LS et al (1978) A coring and squeezing technique for the detailed study of subsurface water chemistry. Can J Earth Sci 15:162–169

Pittari A, Cas RAF, Lefebvre N et al (2006) Facies characteristics and architecture of body 219 Fort á la Corne, Saskatchewan, Canada: implications for kimberlitic mass flow processes in a marine setting. In: Kimberlite Emplacement Workshop Saskatoon, Saskatchewan 7-12 September 2006

Plummer LN, Prestemon EC, Parkhurst DL (1994) An Interactive Code (NETPATH) For Modeling NET Geochemical Reactions Along a Flow PATH Version 2.0. U.S. Geological Survey Water-Resources Investigations Report 94:4169

Remenda VH, van der Kamp G, Cherry JA (1996) Use of vertical profiles of δ18O to constrain estimates of hydraulic conductivity in a thick, unfractured aquitard. Water Resour Res 32(10):2979–2987

Rübel AP, Sonntag C, Lippmann J et al (2002) Solute transport in formations of very low permeability: Profiles of stable isotope and dissolved noble gas contents of pore water in the Opalinus Clay, Mont Terri, Switzerland. Geochim Cosmochim Acta 66(8):1311-1321

Schmeling EE, Hendry MJ, Barbour SL (2012) Hydrogeology of a fractured Cretaceous shale, Fort á la Corne Kimberlite field, Saskatchewan, Canada. In Review

Scott-Smith BH, Orr RG, Robertshaw P et al (1998) Geology of the Fort á la Corne Kimberlites, Saskatchewan. In: Seventh International Kimberlite Conference, Cape Town, South Africa: Abstracts volume:772–774

Shaw JR, Hendry MJ (1998) Hydrogeology of a thick clay till and Cretaceous clay sequence, Saskatchewan, Canada. Can Geotech J 35:1041–1052

Tamers MA (1975) Validity of radiocarbon dates on groundwater. Geophys Surv 2:217–239

Timofeeff MN, Lowenstein TK, Augusta Martins da Silva M et al (2006) Secular variation in the major-ion chemistry of seawater: Evidence from fluid inclusions in Cretaceous halites. Geochim Cosmochim Acta 70:1977–1994

Ugorets V, Pereira C (2011) Groundwater Modeling of Feasibility Dewatering Requirements for Star and Orion South Pits and Possible Hydrogeological Impact. SRK Consulting Inc. Lakewood CO

Van der Kamp G (1992) Evaluating the effect of fractures on solute transport through fractured clayey aquitards. In: Modern Trends in Hydrogeology Hamilton ON 11-13 May 1992 International Association of Hydrogeologists:468–476

Van Loon LR, Glaus MA, Müller W(2007) Anion exclusion effects in compacted bentonites: towards a better understanding of anion diffusion. Appl Geochem 22:2536–2552

Waber HN, Smellie JAT (2008) Characterization of pore water in crystalline rocks. Appl Geochem 23:1834–1861

Wassenaar LI, Hendry MJ, Chostner VL et al (2008) High resolution pore water $\delta^2H$ and $\delta^{18}O$ measurements by $H_2O$(liquid)-$H_2O$(vapour) equilibration laser spectroscopy. Environ Sci Technol 42(24):9262–9267

Wittrup MB, Kyser TK (1990) The petrogenesis of brines in Devonian potash deposits of western Canada. Chem Geol 82: 103-128

Zonneveld JP, Kjarsgaard BA, Harvey SE et al (2004) Sedimentologic and stratigraphic constraints on emplacement of the Star Kimberlite, east-central Saskatchewan. Lithos 76(1):115–138

726 Zonneveld JP, Kjarsgaard BA, Harvey SE et al (2007) The influence of depositional setting and
727 fluctuating accommodation space on kimberlite edifice preservation: Implications for
728 volcanological models of diamondiferous kimberlites at Fort á la Corne, Saskatchewan, Canada.
729 Geological Society of America, Abstracts with Programs 39(6):1–20

730

731

732

733

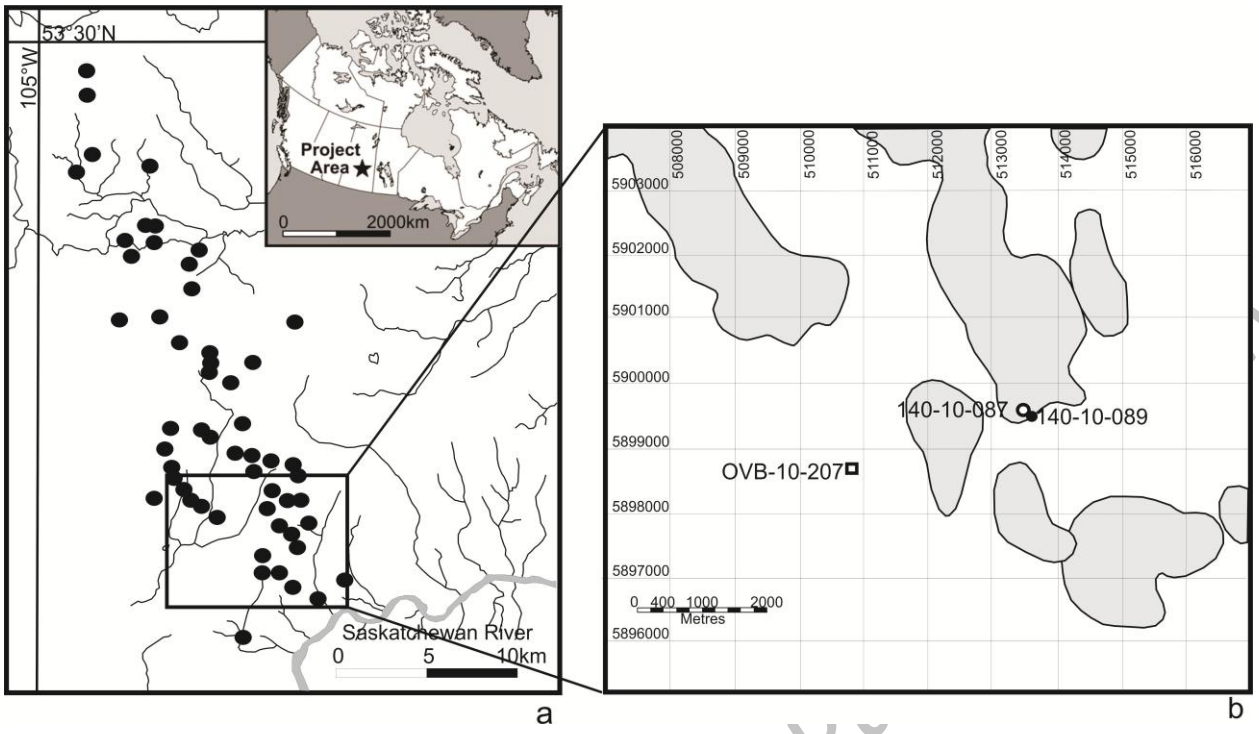


Figure 1. Study area details. (a) Location of the study area and major surface water features. (b) Drillhole locations and major geologic features. Kimberlite bodies are identified by black dots in a and highlighted in grey in b. Drillholes applicable to this study are identified with black dots in b.

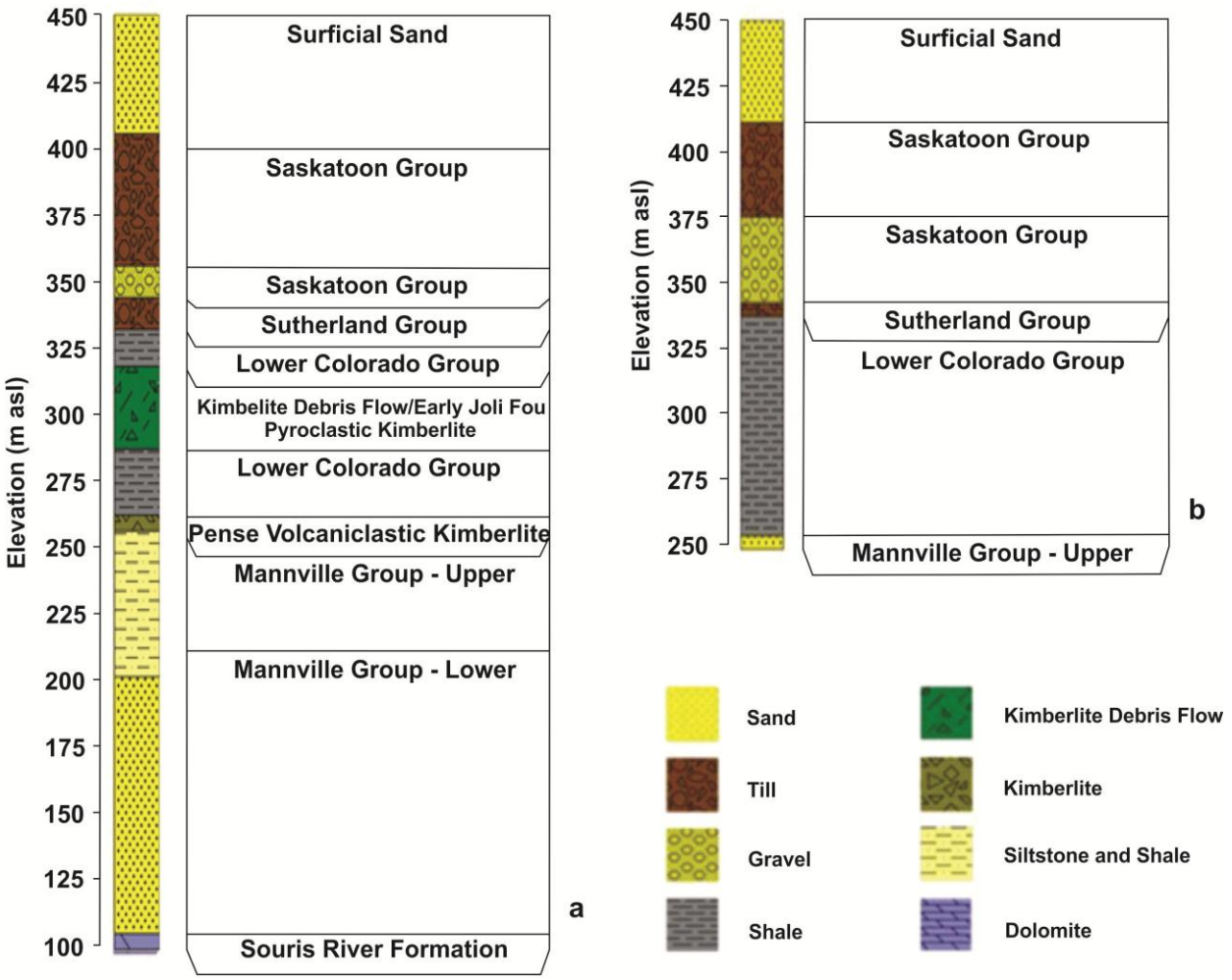




Figure 2. Stratigraphic logs of boreholes 140-10-087 (a) and OVB-10-207 (b).

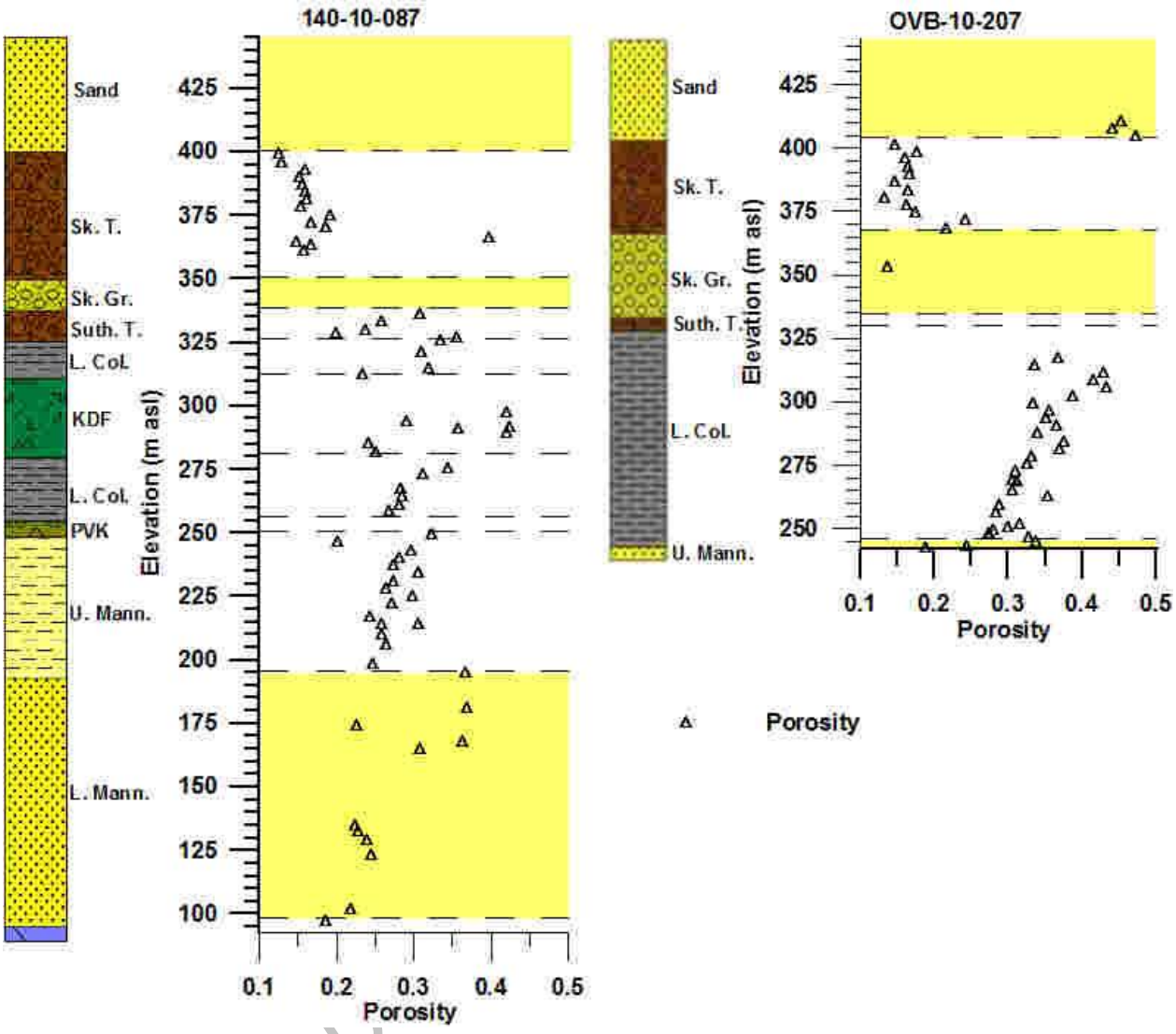


Figure 3. Porosities determined on core samples collected from boreholes 140-10-087 and OVB-10-207.

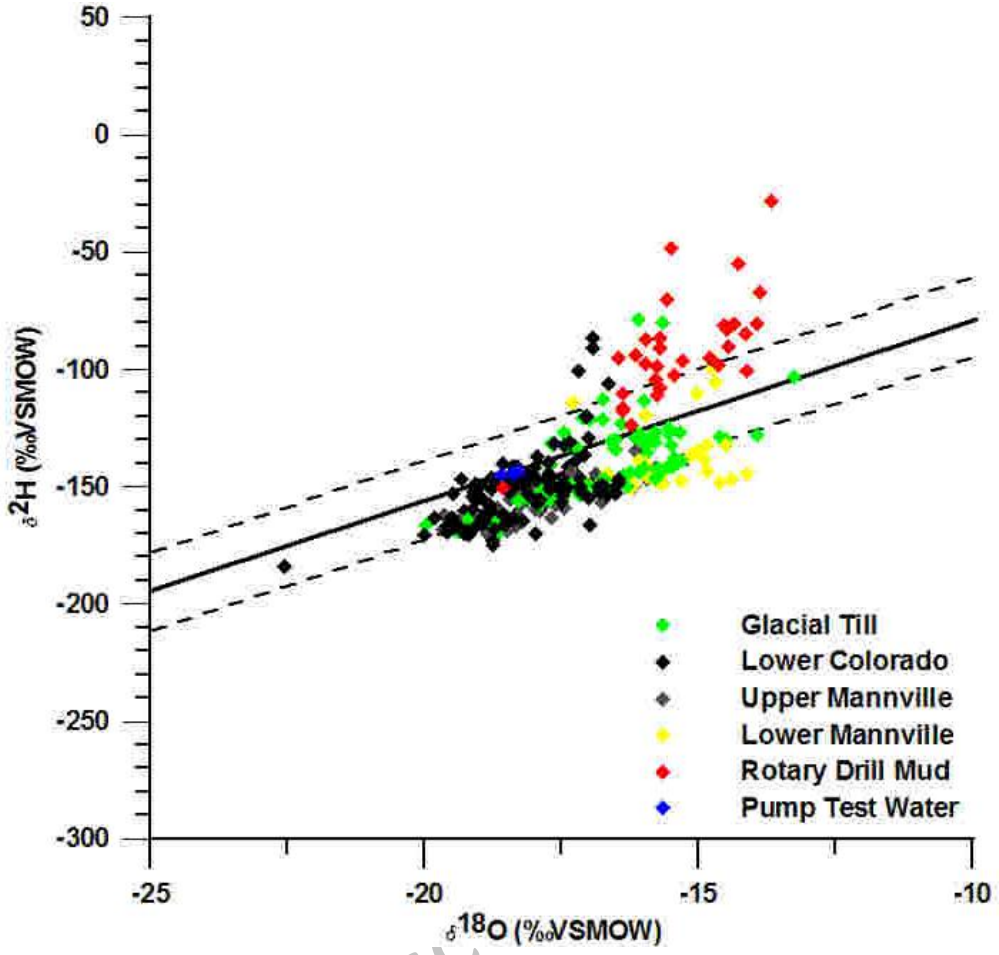


Figure 4. Plot of $\delta^2H$ versus $\delta^{18}O$ for porewater collected from core samples at OVB-10-207 and 140-10-087 and drilling fluid used to core at both drillholes. The solid line represents the Saskatoon local meteoric water line and the dashed lines represent the 95% confidence interval of precipitation data.

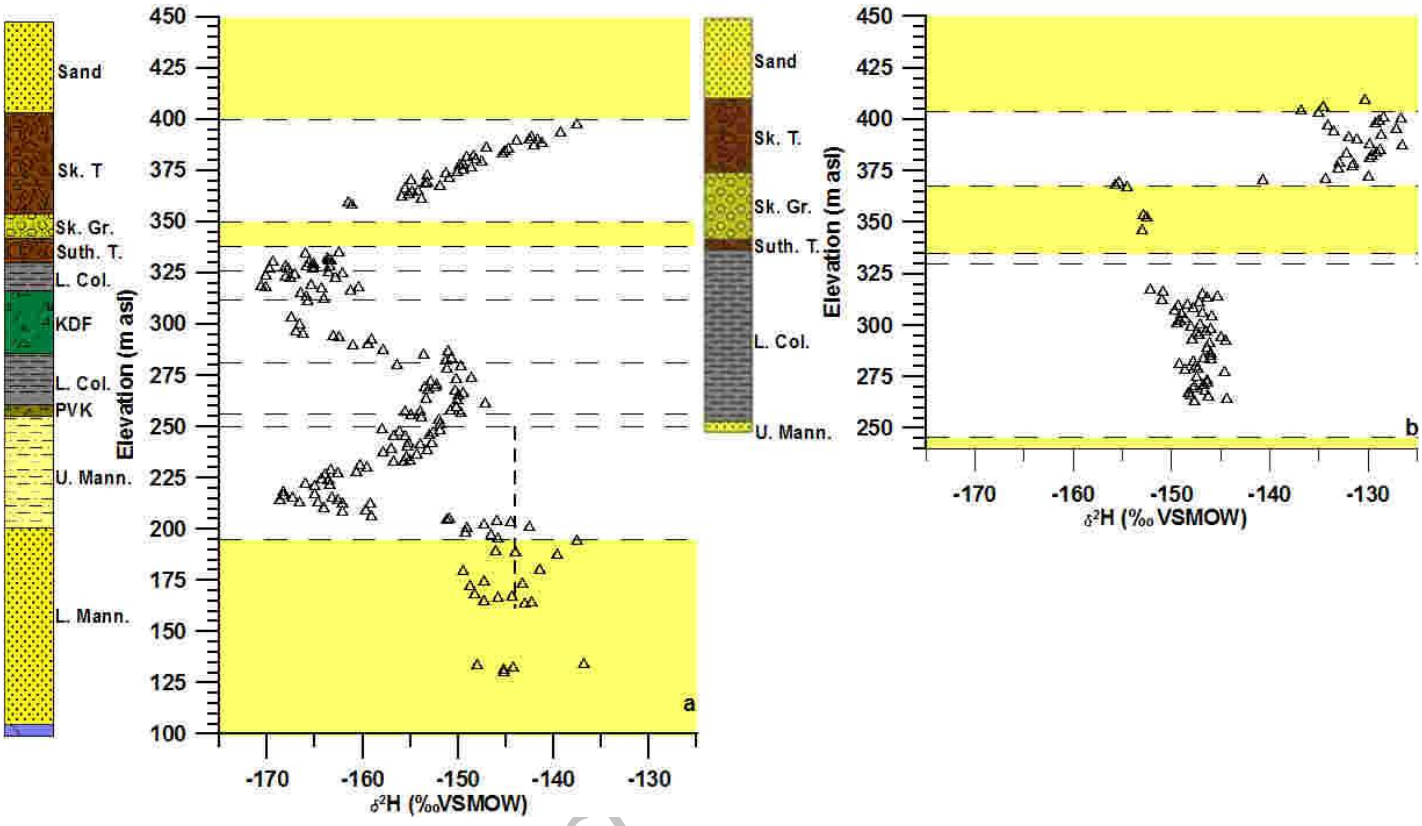


Figure 5. $\delta^2H$ values versus depth through the till and shale aquitard systems and sand aquifer system at 140-10-087 (a) and $\delta^2H$ values versus depth through the till and shale aquitard at OVB-10-207 (b). The vertical dashed line in (a) represents the average $\delta^2H$ value of pump test water collected from a well screened from 195 to 283 m BG. Aquifers are represented by yellow squares on a and b.

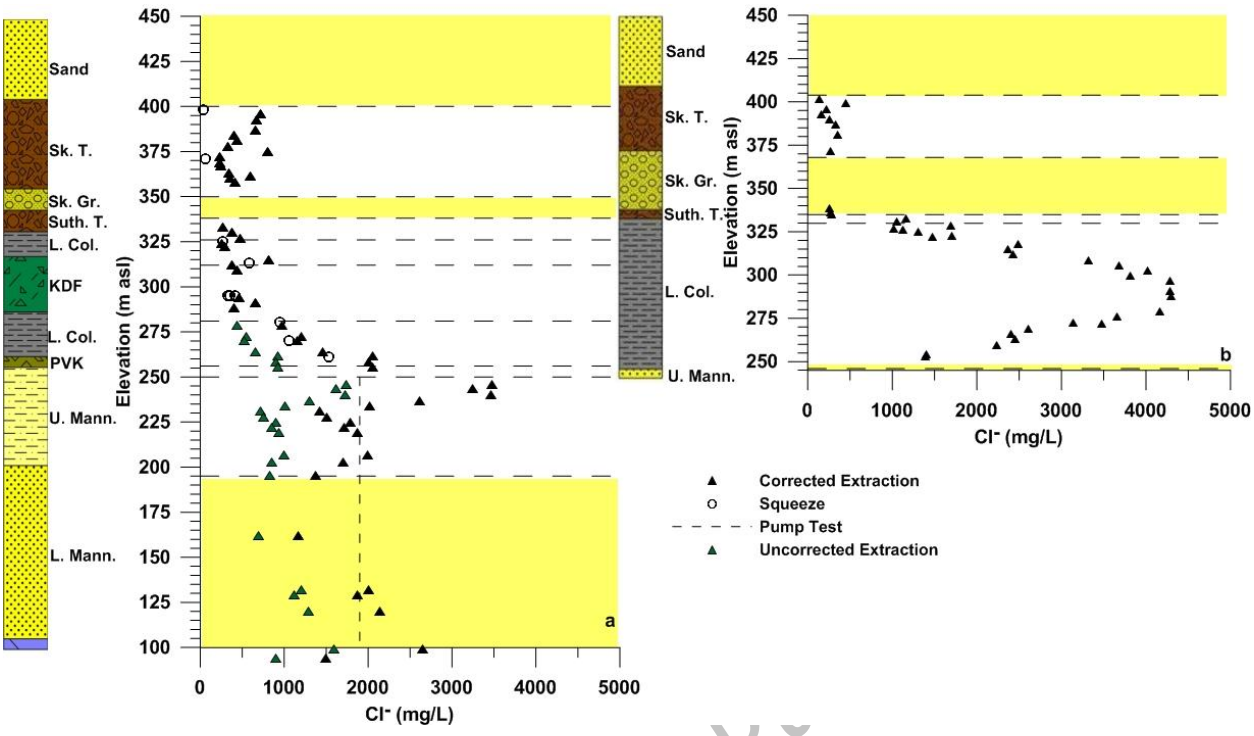


Figure 6. $Cl^-$ concentrations determined from aqueous extractions, mechanical squeezing, and pump test waters for borehole 140-10-087 (a) and OVB-10-207 (b). Porewater $Cl^-$ concentrations were corrected from aqueous extraction data by fitting the extraction data to the squeeze and pump test data by altering the effective porosity for $Cl^-$ in a. The vertical dashed line in (a) represents the average $Cl^-$ concentration of pump test water collected from a well screened from 195 to 283 m BG. Aquifers are represented by yellow squares on a and b.

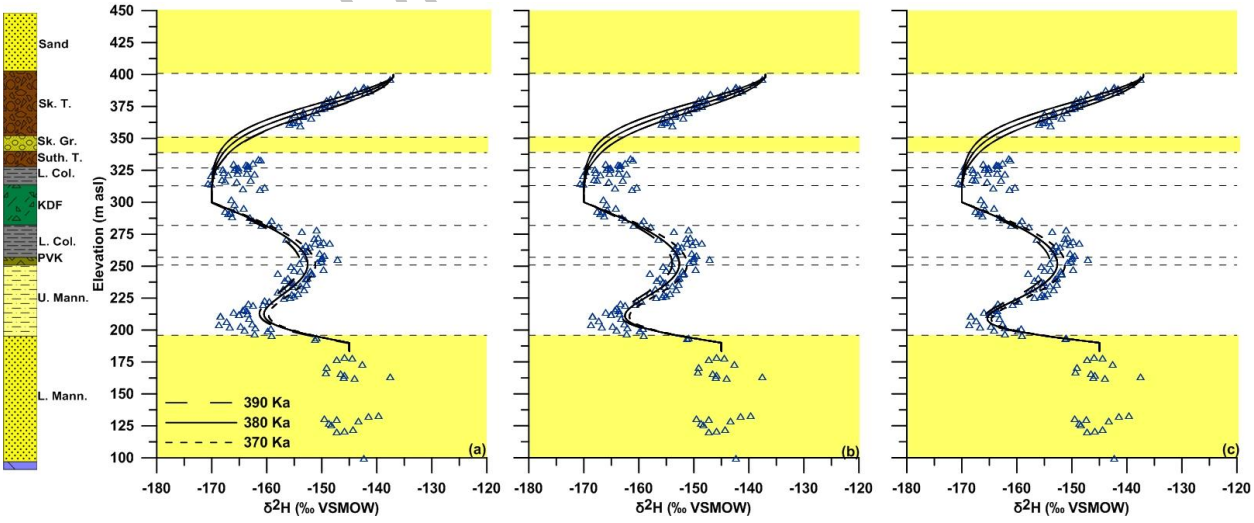


Figure 7. Measured and simulated $\delta^2H$ profiles at 140-10-087 vs. depth through glacial till using downward linear groundwater velocities of 10, 12.5 and 15 m 10 $ka^{-1}$ from left to right. Lower Colorado

and upper Mannville shales were modeled using evolution timings of 390 to 370 ka, represented by dashed lines and a groundwater velocity of 0 m 10 $ka^{-1}$ (diffusion only). Lower Mannville activation times of 20, 15, and 10 ka are presented in a, b and c, respectively. Details of initial and boundary conditions used in the modeling are presented in the text.

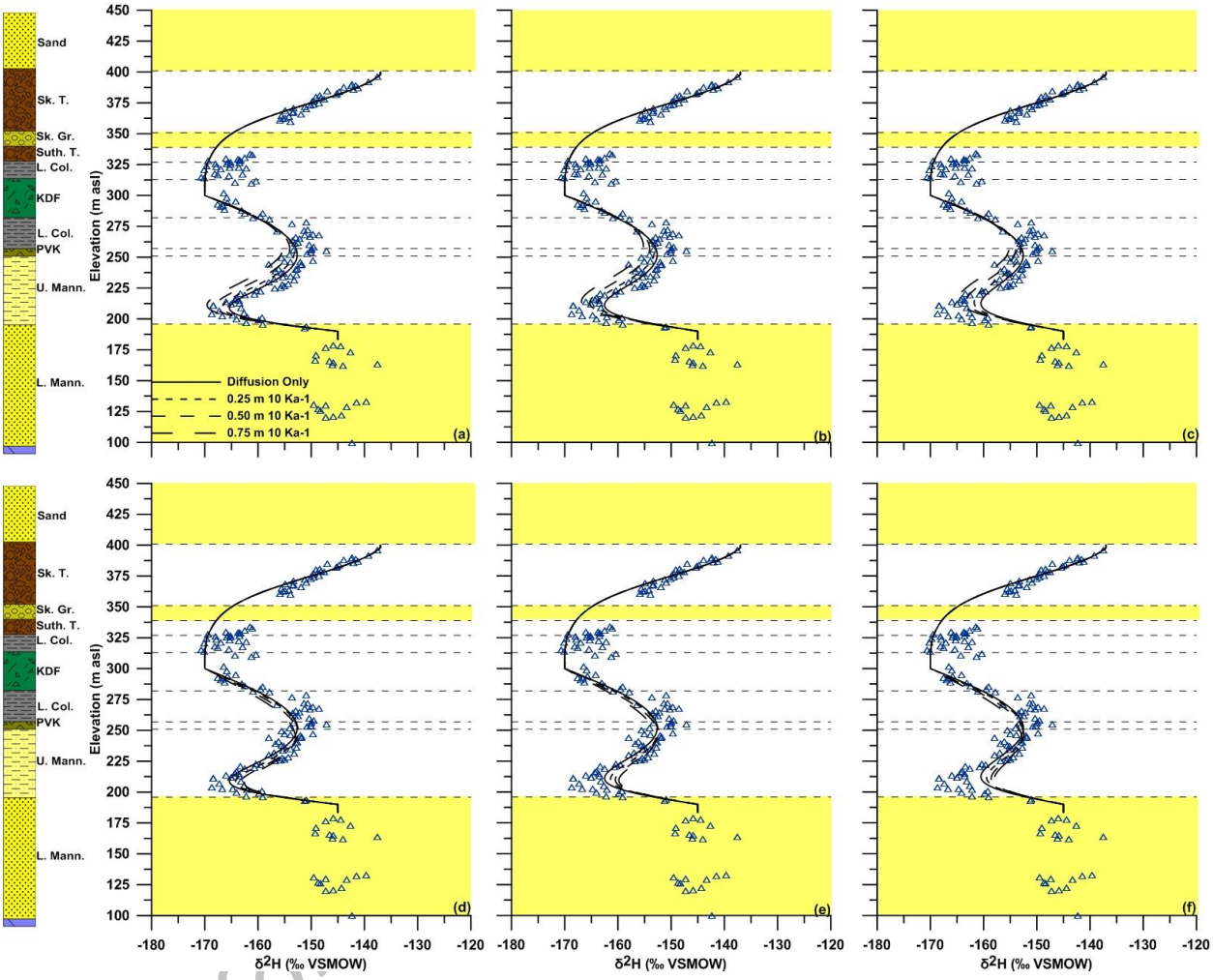


Figure 8. Measured and simulated $\delta^2H$ profiles at 140-10-087 vs. depth using upward (a, b and c) and downward (e, f and g) advection velocities of 0.25, 0.50, and 0.75 m 10 $Ka^{-1}$, represented by dashed lines in a-f, using evolution times of 10 ka in the Glacial till and 380 ka in the Lower-Colorado and upper Mannville shales. Activation times of 10 ka (a, d), 15 Ka (b,e) and 20 ka (c,f) are presented for the lower Mannville. Details of the initial and boundary conditions used in the modeling exercise are presented in the text.

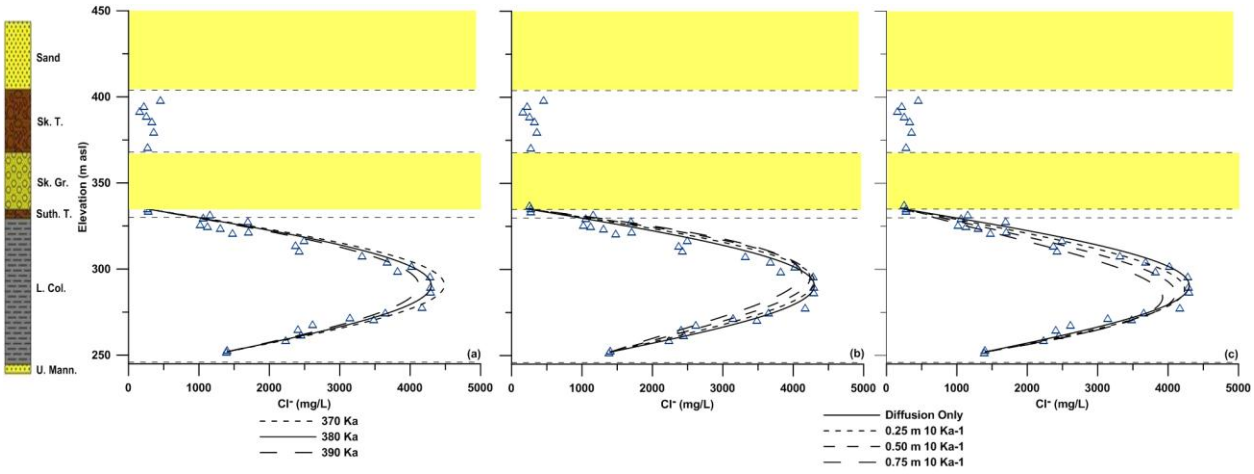


Figure 9. Measured and simulated $Cl^-$ profiles for OVB-10-207 vs. depth. Profiles in (a) were simulated as diffusion only using evolution timings of 390, 380 and 370 ka, represented by dashed and solid lines from left to right. Profiles in (b) and (c) were simulated using an evolution timing of 380 ka, upward linear groundwater velocities of 0.25, 0.50 and 0.75 m 10 $ka^{-1}$ (b) and downward linear groundwater velocities of 0.25, 0.50 and 0.75 m 10 $ka^{-1}$ (c). Details of initial and boundary conditions are presented in the text.

Table 1. Summary of corrected Mannville groundwater ages estimated using $\delta^{13}C$ and $^{14}C$ values from pump test water.

| Model | Age (years) |
|---|---|
| Vogel | 21630 |
| Tamers | 17885 |
| Ingerson and Pearson | 18420 |
| Mook | 15698 |
| Fontes and Garnier | 18876 |
| Eichinger | 17996 |